Experimental Characterization of Automated Fiber Placement Process Defects in Composite Structures

Kaven Croft

Structures and Composite Materials Laboratory
Department of Mechanical Engineering
McGill University, Montreal

August 2010

Thesis submitted to McGill University in partial fulfillment of
the requirements of the degree of Master of Engineering

"Only those who risk going too far can possibly find out how far one can go."

- T.S. Eliot

Abstract

The Automated Fiber Placement (AFP) process has good potential for manufacturing large composite structures and is used for large scale production. However, the AFP process reveals uncertainties associated with the induced defects. This investigation examines the ultimate strength variation induced by a single gap, overlap, half gap/overlap and twisted tow defects. Tests are carried out on three lamina properties (fiber tension, fiber compression and in-plane shear), two laminate properties (open hole tension and open hole compression) and each was compared with a baseline configuration without defects. It is observed that the effects are negligible at the lamina level (less than 5% reduction) compared to the laminate level (up to 13%). In addition, the fiber waviness induced by the defects has more impact on the compression properties due to induced micro-buckling. A global prediction method is finally presented to obtain a model that considers the effects of the defects under investigation.

Résumé

Le procédé de placement de fibre automatisé a démontré un intérêt grandissant pour la fabrication de grandes structures en matériaux composites. Il fait néanmoins l'objet d'incertitudes dues aux nombreux défauts de fabrication. Cette étude se penche sur la variation de la contrainte ultime lorsque des défauts de type écartement, chevauchement, demi-écartement/chevauchement et torsadé sont présents. Des tests ont été éxécutés pour trois propriétés de pli (tension, compression et cisaillement) et deux propriétés de laminé (tension et compression avec un trou non contraint). Les propriétés sont ensuite comparées avec une configuration sans défaut. Les tests démontrent que les effets sont négligeables au niveau du pli (moins de 5%) comparé au niveau du laminé (jusqu'à 13%). De plus, l'ondulation des fibres induite par les défauts est plus néfaste en compression, puisqu'elle initie leur micro-flambage. Pour conclure, un modèle de prédiction global tenant compte de l'effet des défauts est proposé.

Acknowledgements

Table of content

Table of Figures

viii

CHAPTER 1: Introduction

During the last 50 years, a number of industries such as the aerospace, automotive, wind energy, sporting goods and military have worked hard to improve the quality of their products and processes in order to make them more reliable and to obtain advantages over competitors. To do so, companies have often chosen to use advanced composite materials rather than traditional materials because of their high strength/weight ratio, good fatigue life and good impact resistance. The major disadvantage of composite materials is the difficulties they present in the manufacturing process. Compared with conventional materials, enormous labour, and hence labour costs, has often been required to achieve good quality and repeatability, and this is even truer for large productions and large parts. In other words, large parts often need more attention and labour time to achieve the same quality as small parts. Such weaknesses have driven researchers to optimize and develop new processes, with the goal of reducing labour costs, improving efficiency and improving part quality.

1.1 Composite Material Definition

A composite material is based on a mixture of different materials, usually two, to make a single material. The combination of a matrix (thermoset resin, thermoplastic or metal) with reinforcements (continuous fibers, random short fibers, fabrics or metals) results in a material which has, in most cases, orthotropic properties. These properties are sometimes defined using a mixture law, which considers the ratio and the properties of each component. Because the properties (strength and modulus) of both fibers and matrix are not the same, the resulting properties of the composite materials are a mix of these two materials. In other words, a composite material is not as stiff as the fibers and not as soft as the matrix, but depends on the ratio of the two. Therefore, the three main parameters for qualifying composite materials are the reinforcement and the matrix and the ratio of these. The reinforcement material is available in many configurations: unidirectional fibers, chopped fibers and more frequently continuous fibers woven into a fabric. The material properties depend on the

1

orientation of the reinforcement and must be split into three principal axes (orthogonal), which allow the material to be defined along these three axes by its properties. The resulting material is stronger or stiffer when most of the fibers are axially aligned with the load, allowing a better force transmission along the parts.

One of the goals of using a composite material is to create a customized material for a particular application. While satisfying design requirements the fiber orientation can be tailored to maximize strength, stiffness, and the vibration response. For this reason, a composite material is built with several superposed thin layers (lamina) made of matrix and reinforcement, which allows each ply to be oriented independently. This build-up of layers is called laminate. The laminate properties depend on the total number of layers and the particular properties of each lamina, namely, fiber and matrix properties, the amount of each component, the orientation of the fibers, and the position of each lamina in the laminate. The properties of an entire laminate can be calculated using the Classical Lamination Theory (CLT), which consists of finding the laminate stiffness matrices (ABD matrix) and then the laminate properties (E_x, E_y, G_{xy}, n_{xy}, n_{yx}, h_{sx}, h_{xs}, h_{ys} and h_{sy})[1]. In order to find the laminate properties, the required parameters are the engineering constants of each component, the ratio of these components, as well as the orientation and the thickness of each layer. Depending on the stacking sequence, the stiffness matrix can lead to undesirable internal distortions (extensional, coupling and bending) and a reduction of the failure strength. To reduce this impact, symmetry and balance have been defined as follows.

> A laminate is called symmetric when for each layer on one side of a reference plane (middle surface) there is a corresponding layer at an equal distance from the reference plane on the other side with identical thickness, orientation, and properties. The laminate is symmetric in both geometry and material properties[1].

> A laminate is balanced when it consist of pairs of layers with identical thickness and elastic properties but have +θ and -θ orientations of their principal material axes with respect to the laminate reference axes[1].

The equilibrium between plies on each side of a symmetric laminate removes the coupling, or in-plane/flexure, because the same load is equally distributed on both sides. This elimination can be shown on the ABD matrix by removing all B terms, a choice that improves the stability of the laminate under load and after

cure. Basically, an unsymmetrical laminate will have residual stresses that come from the inside bending of plies. This bending influences the stability and the reaction of the laminate under load. Similarly, the balance property eliminates the in-plane shear term of the A matrix. The in-plane shear breaks links between plies; this can create delamination, consequently, removing this term stabilizes the laminate. With this knowledge, designers can create the best sequence for their needs and, with the help of a number of tools (Classical Lamination Theory (CLT), Failure Criteria, Finite Element Analysis (FEA) and Computer Assist Design (CAD), it is possible to know how the part will react and when exactly it will break. After creating and analysing the laminate, the part needs to be shaped and tested to verify the prediction.

Composite materials are sold in many forms: separate components (fiber and matrix), prepreg materials and standard shapes. Separate components must be placed separately during the manufacturing process and attention is needed in order to respect the design requirements (volume fraction, thickness of each layer and fiber orientation). Since this makes difficult to control their properties, separate components are less used than prepreg materials for high performance parts. Prepreg material is a sheet of fiber reinforcement pre-impregnated with a matrix material and sold in one component. The advantages of prepreg material are the high volume fraction of fibers (higher stiffness), the constancy of this fraction and the uniformity of the thickness. Manufacturing a part with pre-impregnated material implies cutting the pattern needed and stacking each ply adequately in a mould. With this kind of material, attention is needed to correctly place each layer and to remove all air bubbles trapped between plies. For both separate components and prepreg material, parts must be shaped into a mould and a cure must to be applied. A cure is a step where heat and pressure are applied to create cross-links (polymerization) in the matrix and consolidates the laminate. On the other hand, standard shapes are parts commercially sold with predefined geometries and already in a solid state. These standard shapes are sold according to the manufacturer tolerances and have limited cross-sections that depend on demand and feasibility.

1.2 Composite Material Manufacturing Processing for Large Production

In the previous section, a short description of composite materials was made for all types of composites: thermoset, thermoplastic and metal matrix. For this research, whose objectives will be defined later, thermoset resin matrix is used. This matrix needs a combination of heat and pressure to polymerize the resin (chemical cross-linking) and to obtain a solid state. The manufacturing methods differ according to the material types, i.e., a separate component or prepreg. Separate components are usually used for large parts whose weight does not need to be optimized and where mechanical properties are not an issue. On the other hand, prepreg is used for hi-tech products because of its high stiffness-to-weight ratio and its precise fiber orientation. In order to manufacture large parts with precision, several techniques have been developed, as summarized below.

Hand-layup is the simplest manufacturing technique for all parts; it has been adopted by many companies and consists of manually stacking each ply in a mould. This technique can be used with both separate components and prepreg material. The advantage of this technique is the low investment in tooling, but the quality is directly proportional to the quality of the labour performing the operation. Both materials are processed in the same way: the worker cuts the fabric and compacts both components, with a hand roller, in alternation, to create the sequence in the mould. As said previously, prepreg material allows tighter tolerances, better product finish and better product performance. Consequently, aeronautic companies prefer using prepreg to using separate components. To reduce the lack of accuracy, companies have introduced automated cutting tables and laser projection markers; the former cuts and optimizes patterns on the sheet of raw material and the lather shows the position of the pattern on complex mould shapes. Consequently, these techniques reduce scrap and time, while increasing accuracy.

After completing the layup, curing is needed in order to complete the process. For large-scale production, two main techniques are available to cure thermoset composites: vacuum bagging and autoclave processing. The choice of a technique is influenced by the material. Vacuum bagging consists of sealing a

bag around the part and removing all trapped air between the bag and the part. Then, the entire set-up is placed in an oven and heated for a certain amount of time; this permits the part to polymerize and obtain a solid state (Figure 1). A variant of vacuum bagging is the use of a closed mould with an internal bladder (heat resistant balloon). In

Figure 1: Vacuum Bagging System[1]

this case, the bladder is filled with air which pushes the laminate on the mould cavity, creating pressure on the part, and heat is applied afterwards. Similarly, autoclave processing consists of a vacuum bagging process, except that the entire process is made in a pressurized oven (autoclave). In other words, a mould with a vacuum bag is inserted in the autoclave and the autoclave is pressurized, adding even more pressure on the laminate. The pressure created is higher than with vacuum bagging; this is better for removing the excess of resin and all the air trapped between each ply. The disadvantages of the autoclave process are the high cost associated with the tooling and the need of filling it with low compressibility gas.

Even with all the new techniques for enhancing productivity and quality, and for reducing errors associated with hand-layup, the disadvantages mentioned above are continuously motivating searches towards solutions and innovations in the manufacturing process. So, companies have introduced new moulding and automated technologies, with higher production rates, such as Resin Transfer Moulding (RTM), filament winding, Tape Laying and Automated Fiber Placement (AFP). All these new technologies will be
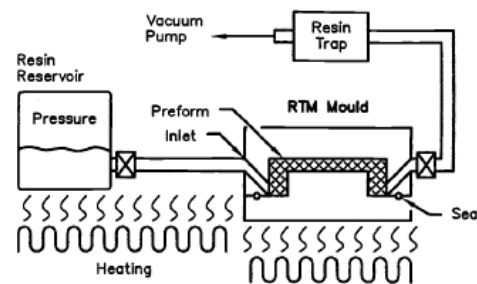
Figure 2: Resin Transfer Molding System[2]

---

[1] Baker Alan, Dutton Stuart and Kelly Donald, 2004, Composite Material for Aircraft Structures, 2nd Edition, p. 125.

[2] Baker Alan, Dutton Stuart and Kelly Donald, 2004, Composite Material for Aircraft Structures, 2nd Edition, p. 133.

discussed in more detail and emphasis will be made on the technology used during this research: AFP.

RTM is a process in which dry fibres (preform) are placed in a closed mould (Figure 2). Then, pressurized resin is injected into the mould inlet and a vacuum is created in the mould outlet (VARTM: vacuum-assisted RTM). When the entire cavity is filled with resin, pressure and heat are applied to cure the part. After the curing process, the mould is opened, the part is removed and the process can restart from the beginning. This process is very efficient and allows a high production rate with low investment. This investment is proportional to the size and complexity of the part and, consequently, to the tooling complexity. Also, careful adjustments of many parameters are needed to obtain good part quality in areas such as fluid flow, injection time, in-mould pressure, detection of risky areas, preform twisting tolerances and shape, and the position and number of inlets/outlets. In addition, because larger parts have larger cavity areas in the mould a higher pressure is needed to fill the cavity and a higher clamping force must be applied to close the mould. For this last reason, large parts need high investment and this process is limited to small and medium-sized parts. Consequently, large structural aeronautic and wind turbine parts are manufactured by other automated techniques.

Filament winding is the oldest automated process and is used basically to create the layup on parts that revolve. This machine consists of a continuous resin-wetted filament (single fibre) that is placed around a mandrel, which is also the mould, i.e. the external
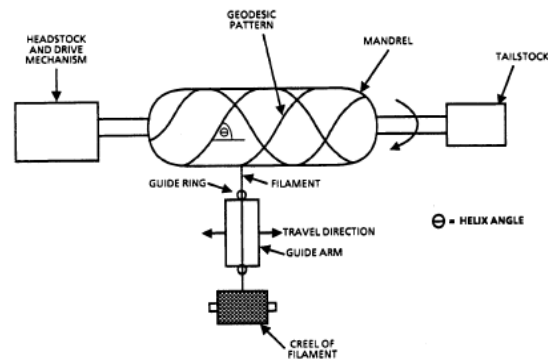
Figure 3: Filament Winding System[3]

shape of the part (Figure 3). The process typically uses a 5-axes machine, which has three translations (x, y and z) and two rotations including the mandrel rotation. One of the fiber ends is attached on the rotating mandrel, which

---

[3] Stuart M. Lee, 1992, Handbook of Composite Reinforcements, p. 341.

stretches the fibre and places it around the mandrel. The computer control robotic arm guides the fiber to obtain the pre-defined pattern shape that constitutes the layup of the part. Afterward, parts must be cured to obtain its final shape and stiffness, and then the mandrel is extracted. This method is more efficient than hand-layup, in other words, it reduces the labour cost and is more repeatable and predictable. However, the laminate presents a high void content that generates rough external surface finish and reduces the aerodynamic properties. Also, the process limits the ply orientation angle, and the part geometry must be convex to avoid fibre bridging. In other words, no mechanism applies pressure on the mandrel to force the fiber to follow the mandrel's shape and, consequently, the part must be always convexe to avoid the fiber bridging. Thus, the parts and mandrel must be designed to allow the removal of the mandrel afterwards [2]. All these disadvantages have led to the development of other automated processes, such as Tape Laying and Automated Fiber Placement (AFP).

Tape laying is also an automated computer control machine process with 3 to 5-axis, more precisely, three translations (x, y and z) and two head rotations (around x and z). The main difference between this process and filament winding is that the tape laying machine lays-down bands of prepreg material (6.35 to 50.8 mm wide) on the mould surface and consolidates them with a compaction roller. In other words, the prepreg bands go through a distribution head that aligns it and then places it on the mould surface. Also, the head heats the material to reduce viscosity and increase tackiness. Then, a compaction roller consolidates each ply together and removes the air traps. Because this process executes the layup on the mould, a cure is needed to complete the parts. The finished parts have the same advantages as filament winding and a better overall quality, without the poor surface finish. Moreover, this process has the ability to cut and restart the material and, consequently, can create ply with all possible angles. However, this process needs smooth surfaces and, consequently, constrains the part's radius of curvature, because the wide bandwidth does not deform very much in two simultaneous directions. This last shape restriction has become an issue in the aerospace industry. To overcome this limitation, manufacturers have decided to introduce Automated Fiber Placement (AFP),

which is an update of the tape laying process. AFP allows better flexibility, better quality (smaller bandwidths and more axes) and adds more design variables. Since, this work focuses on the AFP process, the following section will provide more detail to understand all the relevant issues.

CHAPTER 2: Automated Fiber Placement Manufacturing Procedure

Automated Fiber Placement (AFP) is a relatively new composite material manufacturing process (mid 1980's) which makes companies more efficient and profitable. With high production rate, good accuracy, flexibility and repeatability, this technique is well adapted for large parts, e.g. airplane fuselages or wind turbine blades.

A typical AFP machine (Figure 4) consists of a computer control robotic arm, with a distribution head at its extremity, which lays up composite material on a mould. Machines consist of six to seven computer controlled axes, three translations, two or three head rotations, and one mandrel rotation that allows manufacturing of cylindrical

X-axis (arm crossfeed)
Y-axis (arm tilt)
Z-axis (carriage longitudinal movement)
C-axis (part/mandrel rotation)
I-axis (head yaw)
J-axis (head pitch)
K-axis (head roll)
A-axis (redirect roller angular position)
Q-axis (tow restart linear position)
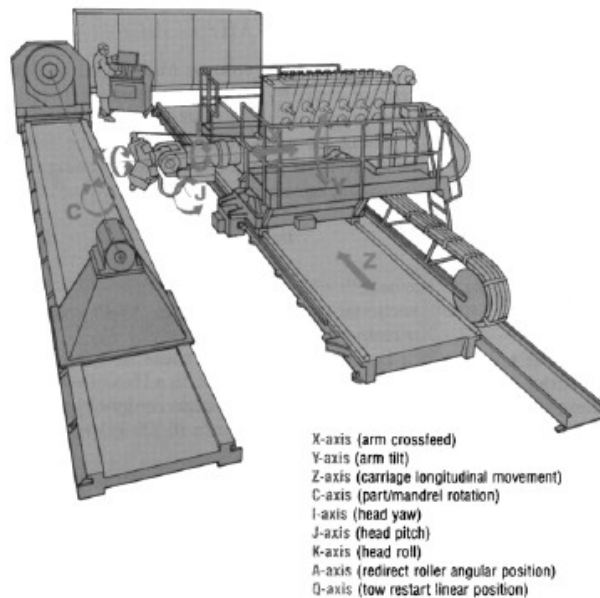
Figure 4: Automated Fiber Placement Machine[4]

parts (mould). The critical part of this machine is the distribution head (Figure 5), which controls the position of the materials, the pressure and the temperature during the ply consolidation.

The material used for this process is continuous bands of prepreg material (0.125" to 0.25" [3.2 mm to 6.4 mm] wide) called tows. These tows are sold in spools and stored on the top of the machine head. They then pass through the guide system of the head, which allows multiple tows to align and form a wide band. Depending of the head configuration, up to 32 tows can be aligned [3]. Wider bands enhance the productivity, by laying down more material; however, they restrain the optimization possibilities by adding more gags/overlaps in the

---

[4] S. T. Peters, 1998, Handbook of Composites, 2nd Edition, p. 477.

laminate (explained in more detail in section 2.2). Each tow is fed individually by the guide, and then a compaction roller stacks them on the mandrel. As a result, the air trapped between plies is removed and the plies are consolidated together. During this step, a hot air system heats the tows to increase tackiness and prevent them from sliding when placed on the mould.
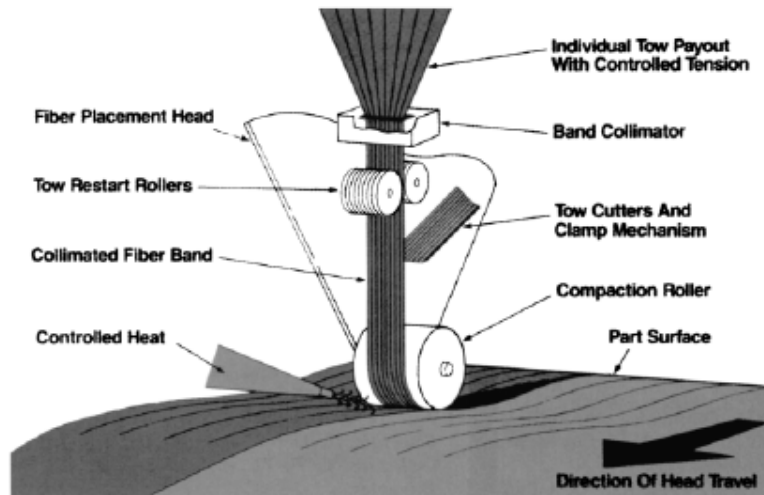
Figure 5: Fiber Placement Head[5]

This process has the ability to create a variable stiffness composite, in other words, to control the change of fiber orientation inside a ply. Variable stiffness composites allow the designer to optimize parts, with better stress redistribution inside the structures. This advantage is made possible by the individual speed control of each tow and the ability to cut and restart them separately. Currently, manufacturing industries of composite materials are positive about the potential gains of using this process, which can bring better quality, improved uniformity, reduction in working time, and better design flexibility. Furthermore, research has proven that the use of AFP generates the possibility of enhancing the buckling load [4-5], reducing the effect of stress concentration [6-7], maximizing the fundamental frequency [8] and improving the impact resistance [9] with an optimization of the variable stiffness in composite structures.

---

[5] S. T. Peters, 1998, Handbook of Composites, 2nd Edition, p. 476.

2.1   Curvilinear Concept

To understand the efficiency of this process in generating variable stiffness composite structures, it is necessary to look at the definition of curvilinear fiber path. Because the stiffness is higher in the fiber direction, the stress distribution in a part is a function of the fiber angle and the stacking sequence. For a variable stiffness composite, the stiffness varies as a function of the part location and, consequently, it is possible to spread the stresses more uniformly inside the entire structure and/or to locally reduce the stress concentration effect. In fact, both the sequence and the angles depend on the parts application and the applied loads. The optimization problem results in being very complex, because many design variables are possible and many geometric factors might influence the solution/s. This complexity is proportional to the parts geometry, so far, only a flat panel, a cylinder and a cone configuration have already been considered as they have simple geometries.
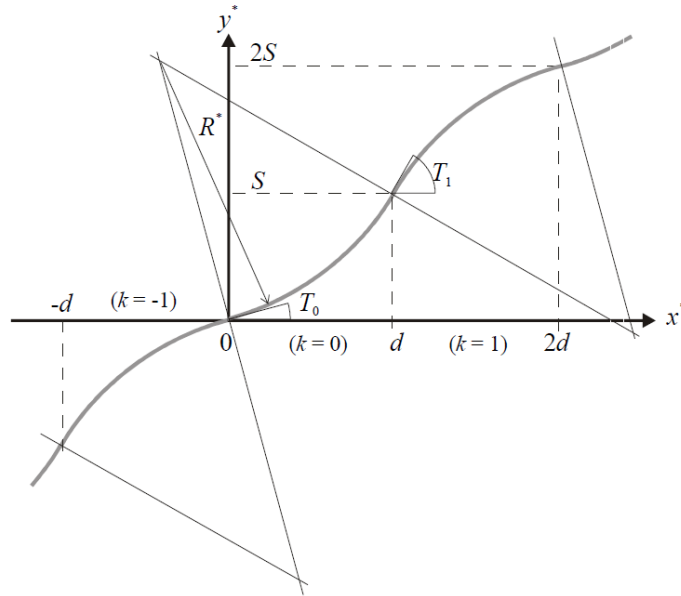
Figure 6: Reference path function for constant curvature [3]

To create a variable stiffness structure, the APP machine lays-down the material following a curvilinear fiber path, which consists of the middle of a bandwidth. Many definitions can be used based on linear variations of the angle. The latest, and more efficient, definition uses constant curvature arc [3], which linearly varies the cosine of the angle to accommodate the constraints (section 2.2) of the AFP machine. Also, this last path definition has the advantage of defining the entire path geometry using six parameters: x_0, y_0, ϕ, T_0, T_1, d. Figure 6 represents the

11

path function for a flat panel of dimension *2d x 2d* in the Cartesian coordinate system, in which the position of the reference path is defined by the x_0, y_0 coordinates. The parameter T_0 represents the angle of the fiber path, according the x-axis, at the origin, and the parameter T_1 represents the angle of the fiber path at the position {*d, d*}. Between these points, the path follows a constant radius of curvature. To include more design possibilities, the variable ϕ rotates the entire coordinate system around the origin. In summary, the reference path definition can be written as the following equation: ϕ<T_0|T_1> [3]. To control the position of all independent tows in a bandwidth and to avoid gaps and/or overlap between tow edges, the machine needs to control the speed of each tow independently. Finally, to cover the entire panel surface, two main filling configurations are used: parallel or shifted.

2.1.1   Parallel ply configuration

The parallel ply configuration is the simplest method as it consists of offsetting all the other reference paths with respect to the first path. In Figure 7, the plane lines represent the reference curve while the dotted lines represent the bandwidth sides. This method constructs panels with all the tow band edges flush to their neighbours. However, to allow
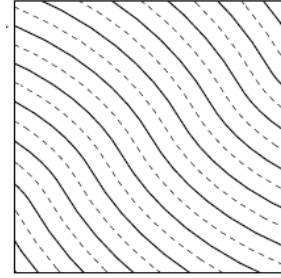
Figure 7: Parallel ply configuration[6]

flush edges, the radius of curvature must be adjusted for each fiber path and at each new position according to the bandwidth. Consequently, the size of the radius of curvature depends on the first reference path and on the location of the subsequent bandwidths; for instance, a large radius of curvature induces a smoother positioning than a small radius of curvature. Furthermore, a radius of curvature below the machine limit tends to wrinkle the tow out-of-plane, which is a kind of imperfection [6]. In general, to lay-down the material with small radius, the machine must reduce its speed, thereby reducing productivity. Sometimes it is almost impossible to build a small radius; therefore, to make sure all fibers will to be placed correctly, a minimum radius of curvature is set on each AFP

---

[6] Brian F. Tatting, 1998, Analysis and Design of Variable Stiffness Composite Cylinders, Ph.D Thesis.

machine. This covering method is restrictive in terms of design possibilities, because the bigger the difference between T_0 and T_1, the smaller the radius of curvature. Thus, with a large panel it is easy to reach the minimum radius of the machine because each bandwidth influences its neighbours.

2.1.2 Shifted ply configuration

A shifted configuration allows more design variables and higher stiffness variations than the parallel configuration. This is possible because all courses are shifted with a constant distance (Figure 8), which maintains the same potentially optimum definition as the first reference path. This implies that there are no changes in angle and radius when compared
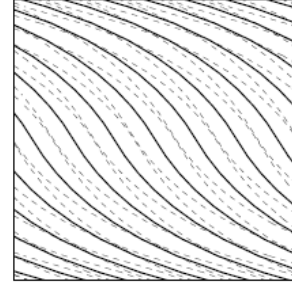
Figure 8: Shifted ply configuration[7]

to the original path. Also, the shifted ply configuration does not influence the tow edges inside the bandwidth, which remains aligned, because it is induced by the placement guide. However, each tow definition inside the bandwidth differs from the reference path (located in the middle of the bandwidth) because of the adjustment made to fit the tow edges inside the bandwidth. Consequently, the bandwidth edges will not fit with their neigbours, creating gaps and/or overlaps depending on the shifted distance. To reduce the size of the gaps/overlaps, the machine head has the capability to cut, drop and restart each tow strip separately. In other words, the machine cuts the tows to reduce the gaps/overlaps at the boundaries of the other bandwidths. Also, the machine head controls the percentage of gaps/overlaps at the boundaries as a design variable. After curing, the gap regions consist of resin-rich areas that reduce the material properties of the entire laminate and eventually can cause delamination [3]. The overlap regions are extra plies that can improve stiffness. Furthermore, they create thickness variations that locally unbalance the laminate and add instability. In several applications, overlap regions can improve buckling load by redistributing the stresses inside the structure. On the other hand, overlaps are not welcome when both appearance and aerodynamic issues are required. Even

---

[7] Brian F. Tatting, 1998, Analysis and Design of Variable Stiffness Composite Cylinders, PhD Thesis.

if variable stiffness is not yet accepted by companies because of the certification constraints, this last covering technique gives more advantages and possible improvements compared to the parallel configuration.

2.1.3   Variable Stiffness considerations according CLT

The prediction of variable stiffness composites with curvilinear fibers is not as straightforward as with straight fibers. The material properties change constantly and to calculate them, the surface must be subdivided into smaller surfaces. Then, the material properties can be found separately for each small surface with the assumption of straight fibers. The combination of all surfaces gives the properties of the entire part; consequently, the overall precision is related to the

number of surfaces, which makes the stress analysis quite complex. The symmetry property is similarly defined as for the straight fibers and does not need additional plies. On the other hand, a variable stiffness laminate without defects needs two more plies to define the balancing property (Figure 9). As explained in section 1.1, balancing plies involves using mirrored plies, which is straightforward for unidirectional fibers. In the case of curvilinear fibers, one mirror is not enough to complete the balancing because fibers vary with each axis (x and y). For this reason, four total plies are needed to fully balance one ply of a curvilinear laminate. This can be written as follows: $\pm\phi\pm<T_0|T_1>$ [3].
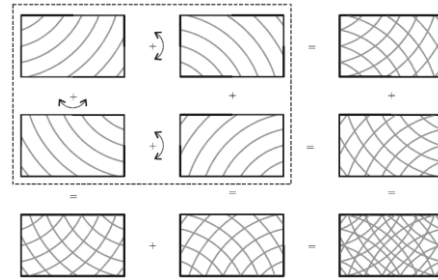
Figure 9: Balancing of plies with variable stiffness[3]

Another issue with the variable stiffness composite is the thickness variation. The thickness variation created by gaps, overlaps and twisted tows (explained in more detail in section 2.2) leads to a locally asymmetric and unbalanced laminate. The part design needs to carefully consider the ply sequence to limit the internal disturbance of the in-plane extension and shear stiffness coupling terms. Consequently, the position of the thickness variation (defect) influences

locally the material properties. Also, the laminate symmetry depends on the stacking sequence,
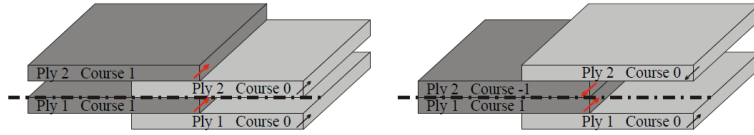
Figure 10: Courses layed down with overlap[3]

as shown in Figure 10 for an overlap configuration, where the left figure is non-symmetric whereas the right figure is symmetric. Another phenomenon that affects the symmetry of the laminate is the local misalignment of the

Figure 11: Ply misalignment[3]

plies around the middle axis plane (Figure 11). This problem is present in the entire laminate and is caused by the mould constraint; in other words, the machine places layers on the mould and compacts the material which creates one flat side and the other rough. Thus, the sequence starts at the bottom and as soon as a change appears in the number of plies, this phenomenon occurs (Figure 11: right configuration).

2.2 Manufacturing Defects

Several kinds of defects occur during the manufacturing of variable stiffness parts; the more common types are gaps and overlaps. These defects are created at the junction of two consecutive bandwidths. The amount of these defects can be adjusted by the process itself with the help of the independent tow cut and restart option. This method allows a better control of the defects, but the shapes and sizes are dependent on the geometry and tow width. The defects have been demonstrated as having influence on the mechanical properties and a better understanding of these influences should help to develop better designs. However, an investigation can be very complex because gaps and overlaps play different roles depending on the laminates and the applications. Figure 12 illustrates the complex relationship between the process and the defects, which can form a basis for a possible test plan. From a manufacturing point-of-view, even without the variable stiffness, gaps and overlaps occur all the time due to the process instability and tolerances (tow, machine and process). Other defects can occur during the manufacturing, such as, twisted tow, fuzz, splice and bridging tows. A twisted tow is when a tow rotates or "twists" by a full 180°, in

other words, the tow locally flips upside down. Fuzz is a defect created by the guide dust (short fibers), which sticks on tows before to be laid-down. A splice is a material-related defect, which consists of the end-to-end tows bonding in order to create a longer tow. A bridging tow appears when a tow does not bond on a concave surface and can be avoided with good process parameters. For the operator, all these defects lead to a big question: Do we need to repair the defect or not? This question motivates several researchers to understand the influence of the defects subjected to several different loading scenarios. In fact, each defect creates perturbations in the laminate that may affect its performance, which can be different for each loading case. Also, multiple defects bring other questions about their combined influence, which may be function of the number of defects, the defect size and the defect position. Depending on the application, the effect of all of these parameters can be explored under different conditions, such as with different stress concentrations, thicknesses, layups, materials and loading cases.

After a description of the research goals (section 2.3), a Literature Review (section 3) will present an overview of composite materials defect characterization for materials manufactured using the advance fiber placement process.

**Automated Fiber Placement
(Manufacturing Considerations)**

Machine Contraints

- Minimum radius of curvature
- Fiber orientation range
- Speed
- Compaction pressure
- Path tolerance
- Path definition: $\emptyset <T_0 \mid T_1>$

Parallel Fiber Path
- ↓ Design Possibility

Shifted Fiber Path
- ↑ Buckling resistance

Defects: Gaps, Overlaps and Twisted Tow

- Failure initiation
- Uneven surface
- Strain Perturbation

Asymmetry

- Effect on the coupling matrix (Bending effect)
- 3D Effect (out-of-plane waviness)

Number of Defects

- One defect have a significant effect on mechanical properties
- Defect through the with is more damageable than through the length

Defect Size

- Any defect size have an impact on properties
- reduction is more relevant for the first 0.03"

Defect Position

Lamina / Laminate Properties

Stress Concentration

Laminate Thickness

Method to reduce the impact of the defects

- Interweaving: Better distribution of the defects and thickness (Offset all tows paths at each layer)

- 1st and Nth plies made with ±45° unidirectional fibers:
  ↓ Crack propagation
  ↓ Effect of residual stress
  ↑ Impact resistance
  ↑ Smooth outer surface

Figure 12: AFP Manufacturing Defects Considerations [3, 10]

2.3 Goal of this Research

This research is part of the Consortium for Research and Innovation in Aerospace in Quebec (CRIAQ) COMP413 project. The ultimate goal is to create an optimum composite structure using tow steered design via characterization of Automated Fiber Placement (AFP) induced defects. To arrive at this ultimate goal, the project is divided into three parts. First, experimental characterization, prediction models and non-linear finite element analysis (FEA) of different kinds of defects are needed to understand and quantify the impact of the manufacturing defects induced by the AFP process. Second, considering the previous results, a numerical optimization model will be built in order to optimize the curvilinear fiber path of each laminate layer. The third phase will consist of using the previous phases to design an optimum and complex aeronautic part in order to show the reliability and the possibilities of this manufacturing process.

The present research is situated in the first phase of COMP413 and focuses on the experimental characterization of defects and their effect on the main mechanical properties required by aeronautic companies. Therefore, tests and micrographs on samples, with and without defects, will be executed to compare the effect of each type of defect. Both lamina (layer properties) and laminate (failure criterion) properties are needed for designing and predicting part behaviour. Micrographs, on the other hand, will help in the understanding of the fracture mechanism and will help examine the internal geometry for defects, i.e. out-of-plane waviness, delamination, air bubbles and unpredictable gap/overlap. By combining the results from the mechanical properties and the micrographs, a clear picture of the behaviour under load and a comparison among all the specimens will be drawn.

As said previously, the defect configuration possibilities are numerous; reproduce all of them is an unfeasible task. For this reason, during this first phase of testing, defect configurations are restricted to one tow gap, one tow overlap, one tow half gap/overlap and one twisted tow, which are then compared with a non-defect baseline configuration. Moreover, all configurations will be tested on three lamina properties (fiber tension, fiber compression and in-plane shear strength) and on two laminate properties (open-hole compression and open-hole tension strength).

The final step consist of proposing a plan for future experiments to obtain the range of the defect's impact. This plan will focus on how the defects are distributed through the thickness. According to the literature, a three-defect configuration (45°, -45° and 90°) is likely to be the worst-case scenario; thus it will be described here. To increase defect density, half of the layers will contain defects (gap or overlap), which should spread the effetcs throughout the entire thickness. In addition, from the results of the previous tests, the compression and open hole compression test will help to provide a guideline for future research. Finally, a global prediction method, considering the impact of each defects will be described to facilitate the analysis and the optimization of complex AFP structures with accuracy. This work should provide a baseline for future research on larger specimens, subsequent analysis and establishes a set of pre-qualification data.

CHAPTER 3: Literature Review

Since the introduction of the AFP process in 1990 [11], the potential improvements that variable stiffness structure can bring about have driven researchers to focus on how to exploit the AFP capabilities. Several studies and methods are available in literature to describe the performance of variable stiffness parts. However, all these models do not consider the defects induced by the process which, naturally, should affect the material properties of the laminate. The misunderstanding of the real impact of the internal defects does not allow an efficient use of the new advantages inherent to this manufacturing method for an optimum product design. These defects are difficult to predict because they appear randomly inside an entire structure which has a variable geometry. Furthermore, the defect's impacts should vary between all type of materials, due to the different chemical composition, and the different laminate architecture. For this project, the chosen carbon-epoxy material (defined by our industrial partner) is different than that used by other researches found in literature. Consequently, the conclusions from the literature cannot be applied directly, but can be used as a guideline for comparison, better understanding and further investigation. This section summarizes and compares previous research studies in order to define the approach that will be adopted in this work.

3.1   Previous research

Experiments at the Bell Helicopter Textron facility conducted by Ronald Measom and Kevin Sewell [12] has shown that bandwidth sizes (0.500, 0.75 and 1.000 inch [12.7, 19.1 and 25.4 mm]) have little effect on the interlaminar shear stress in a flat panel (less than 5 ksi [34.5 MPa]). They demonstrated that the thicker is the ribbon (consequently stiffer), the easier is to push it through the placement head. Their experiments consisted of manufacturing a complex-shape part for each bandwidth size using different cut-and-restart options: full gap, half gap/overlap and full overlap. With all these tests, they concluded that the larger is the bandwidth, the larger the defects will be. This investigation gave results for interlaminar shear test responses for each bandwidth size and for all cut-and-restart configurations. These tests suggest that the overall response is only slightly affected by the cut-and-restart option (less than 10% variation) and not

much more between the different bandwidth sizes (less than 15% variation). They concluded that the gap configuration has equivalent strength as that for hand-laid tape. Unfortunately, these tests did not cover bandwidths of 0.125 inch [3.2 mm] wide, which are currently used in Automated Fiber Placement machines.

Even if the overlap has shown to be potentially beneficial, the gap configuration has seen more development because it is more difficult to predict. The gap creates resin rich areas where cracks can grow easily, but this local in-homogeneity causes less strain perturbation than an overlap [7]. Hugh L. McManus and Yew-Po Mak [9] have found that the stress failure of the unnotched tow-placed coupons show no strain rate sensitivity, which should be different with the introduction of a defect due to the strain perturbation associated with the defects. Concerning the impact of internal defects, A. J. Sawicki and P. J. Minguet [10] have looked at the effect of the intraply overlaps and gaps upon the compressive strength of a quasi-isotropic laminate. They focused on both unnotched and open-hole compression samples made with a standard AFP machine (0.125 inch [3.2 mm] tow wide). They concentrated on compression testing because it is more sensitive than tensile testing. To create the defects in the laminate, they modified the middle layer, allowing gaps and/or overlaps of 0.00-0.10 inch [0-2.54 mm] wide (Figure 13). They concluded that all defect sizes have an influence on the laminate strength reduction. However, this reduction is more relevant for the first 0.03" [0.76 mm], and then the decrease is less pronounced. The compression strength reduction
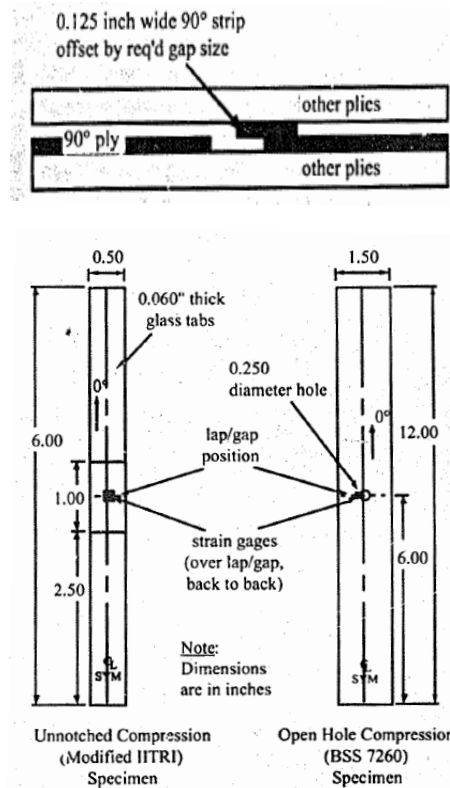
Figure 13: A. J. Sawicki and P. J. Minguet[10] specimens

for unnotched and open hole specimens were similar, which shows that the 0° ply waviness causes by the gap/overlap is the most important sources of strength reduction. As the number of wavy plies increases, the out-of-plane effect increases too, consequently, it increases the interlaminar shear stress and reduces the strength. They have also concluded that a single defect is enough to cause a significant strength reduction depending upon the environment (5 to 10%) and it is consistent regardless of the number of defects. The fracture mechanisms that appear locally next to the defect are mostly matrix-dominated and, consequently, are more sensitive to environmental conditions (hot temperature and high humidity).

Adriana W. Blom et al [13] made a numerical investigation of the progressive compression failure that shows the impact of the tow-drop areas on the stiffness and strength of variable-stiffness laminate panels. Their model consists of a flat panel 30cm x 30cm with a shifted curvilinear fiber path subjected to compression on one axis (Figure 14). The use of the shifted curvilinear fiber path implies that cut-and-restart tows must be performed in order to reduce the
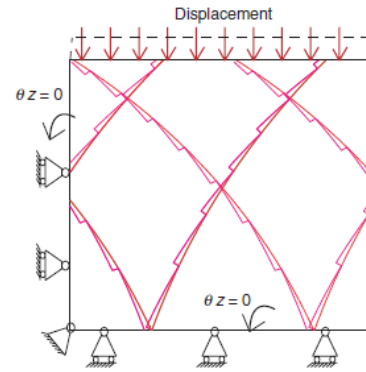
Figure 14: Adriana W. Blom and al [13] model

gap and overlap type of defect along the edges, as explained in section 2.1.2. This method cannot compare the results with a perfect panel without defects and can only give an overview of the global impact of the drop-off parameter. They concluded that both the strength and the stiffness decrease when the number of tows per course increases (8 to 24 tow width per courses), a result consistent with A. J. Sawicki and P. J. Minguet [10]. In fact, a narrow bandwidth has a smaller increment between two subsequent paths and, consequently, the tow-drop areas are smaller, which lead to a smaller impact on the laminate. In addition, the impact on the panel stiffness was found to be proportional to the amount of tow-drop-area. In the case of linear fiber path, the bandwidth dimension does not affect the strength because the tow-drop option is not used. They concluded that the damage is initiated at the tow-drop location and at the higher fiber angle positions. Furthermore, cracks propagate more easily in the external layers than

in the middle layers because the middle plies are constrained by the others. Consequently, the position of the tow-drop area influences the strength and the stress distribution. The overall conclusion is that the staggering method is suitable for smooth surfaces because it creates a better stress distribution regardless of the tow-drop option.

E. V. Iarve and R. Kim [14] confirmed the previous results by doing a three-dimensional numerical and experimental analysis of a discontinuous tow reinforced composite, for which the energy release rate and the possible damage accumulation modes from a tape strip end (Figure 15) were examined. Similarly to W. Blom and al [13], they found that a larger cross-section tow results in a higher energy release rate, and then lower loads are required to cause delamination. The initial failures were found to be located in the resin-rich areas at the tow ends. They concluded that the failure initiates by a
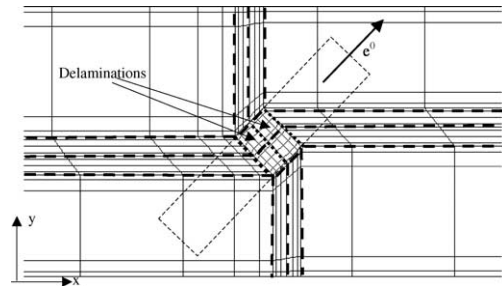
Figure 15: E. V. Iarve and R. Kim[14] model

delamination of the top plies (peel off) followed by the other plies. This explains the high strength retention ratio of quasi-isotropic laminates. They suggested to place a ±45° plies at the top and bottom layers, because these plies can be empty of defects, in order to provide less constraint in the fiber direction and to reduce the residual stress.

Luke Everett Turoski [15] carried out experimental and numerical tests to investigate the impact of the number of gaps on the tensile and compression strength. A model was created with a quasi-isotropic layup in order to compare the impact of the gaps on specimens with and without stress concentration. Three different configurations were investigated, as shown in the Figure 16: unnotched (without centered hole), open hole with a centered defect configuration and open hole with an offset defect configuration. For each configuration, tows were removed to create different gap arrangement: one, two, three and four gaps. For example, the two-gap configuration modifies all layers containing two specific ply angles throughout the entire thickness. The tensile experiments have shown a decrease of about 15% in the failure stress for the

unnotched with three gaps configuration compared with the perfect specimen. However, the open hole tension with three gaps configuration has seen no decrease in strength compared with the baseline. The results from the tension experiments showed that the gaps on the laminate have a smaller effect than the hole and explained the constant strength behaviour of the notch configuration. For the compression tests, both notched and unnotched specimens yielded a failure stress reduction as the number of gaps increases (between 3-11%). In addition, the unnotched configuration is more sensitive to gaps than open hole compression and overall the compression test has more variations compared to the tension tests. The numerical experiment confirms that the offset configuration produces a 12% decrease of failure load compared with the centered configuration. This gap offset unbalances the fiber distribution around the hole, which changes the rigidity on both sides of the hole. Consequently, one side is more loaded and prematurely induces the failure. They also observe that the zero degree ply (through the width) is the one that fails first, and that the one-gap configuration increases the stress concentration compared to the other configurations (which generally spread it instead). The comparison between the experimental and numerical study shows a small increase in the experimental results that can be explained by a small bending of the specimen during the test and the out-of-plane waviness of the fibers, which is caused by the thickness variation induced by the defects.
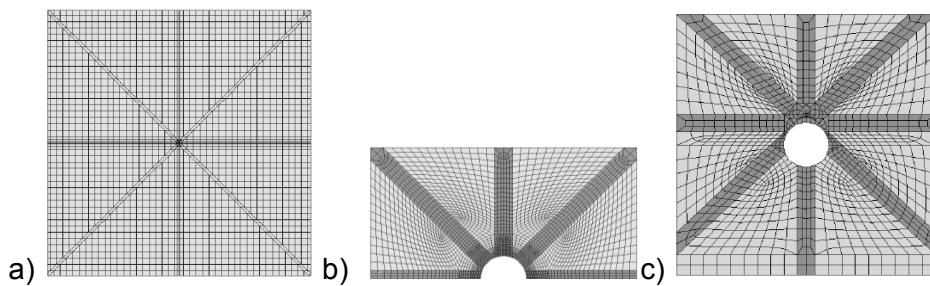
Figure 16: Luke Everett Turoski[15] model a) Unnotched b) OHC with centered defects configuration c) OHC with offset defects configuration

3.2   Approach of this study

This investigation will help to understand the performance of the chosen material with manufacturing defects. As previously described, a good choice of defect configurations is essential because it is impossible to characterize all of the possibilities. Furthermore, an experimental analysis has been set up to look at different defect configurations that will eventually lead to a qualification process, an important step for our industrial partners. A good quantity of samples will accurately reveal the influence of the defects. Therefore, it is not necessary to compare these results with a numerical analysis but can help for future numerical validations of the model. First, a good understanding of a one defect configuration mechanism should be investigated before examining other possible defect configurations that yield the basic failure mechanism. Furthermore, the conclusions of this basic analysis will help to capture the impact of induced defects on relevant mechanical properties, the configurations and the tests sensitivity for each defect. Then, it will be possible to create additional tests that will relate to the worst scenario and will allow a better comprehension of the AFP process. The experiments will be discussed and analyzed in more detail later on and then compared with the literature in order to find correlations. Finally, a relation will be made between the tests and an analytical model so as to include them in a design optimization framework.

CHAPTER 4: Tests Descriptions, Standards, Methodologies and Properties

This section describes in detail all the mechanical tests and the execution without considering the defect configurations, which will be addressed later in section 5.1. First, the statistical approach and the description of the material used will be presented. Then, all mechanical tests will be described together with a review of the mechanical properties and the explanation of the different data acquisition methods. Each mechanical test is governed by a different ASTM standard, which, for a given specimen geometry, recommends the choice of the test parameters, the appropriate fixture, and the strategy to reduce the variability between coupons.

4.1   Test Methodologies

Every test is performed using a hydraulic testing frame (MTS machine) with different coupon geometry that depends on the specific mechanical test. Each defect configuration will be discussed in more detail in section 5. For statistical purposes, five identical specimens are tested for each defect configuration and the final mechanical property is calculated using the average of all these specimens. The average for all five similar coupons, for each type of defect, is calculated as follows:

$$\bar{x} = \frac{1}{n}\left(\sum_{i=1}^{n} x_i\right) \qquad \textit{Equation 1}$$

In this expression, the average is represented by $\bar{x}$, while the term x_i represents the result for the ith specimen and the term n is the number of specimens, i.e. five in this case. A more precise average is usually obtained by increasing the number of specimens. In this case, five is the minimum number of specimen required by the ASTM standards to obtain statistically meaningful values of the properties for each defect configuration. This average gives an accurate value for the experiments, but without providing information about the sensitivity of the tests. The accuracy of the test is represented by the variation between all the specimens and gives a good indication about the validity the test. In the following

26

expression, the test sensitivity is represented by the standard deviation (s_{n-1}) and illustrates the variation between specimen results. The standard deviation is also an indicator of the error between the tests; hence, a small deviation indicates a small error. Similarly, the samples' coefficient of variation (CV) represents the percentage error with respect to the mean:

$$s_{n-1} = \sqrt{\frac{\left(\sum_{i=1}^{n}(x_i - \bar{x})^2\right)}{n-1}}$$

Equation 2

$$CV(\%) = \frac{s_{n-1}}{\bar{x}} \cdot 100$$

Equation 3

This investigation examines the material strength which is associated with the failure criterion, an important design parameter. According to the different material axis (three for an orthotropic material) and configurations (layup, notch, constraint, etc.), the laminate properties change and, consequently, the effect of the defects would be different for all axes. To verify the influence of the defects on the strength, different laminates will be created according to standard methods and tested along the proper axis. The defects will be placed on the middles plies, which reduce the bending and the coupling influence of the asymmetry. Also, micrographs of each defect will be performed to confirm its geometry after cure and to compare them with the predictions and the existing model. The detail of the each defect configuration will be discussed in more detail in section 5.

4.1.1   Material Used

The chosen material is the CYCOM® 5276-1 from Cytec Engineered Materials Inc. This material is a unidirectional carbon/epoxy prepreg with a tough resin system. Each tow comes in a spool and is 3.175 mm (0.125") wide by 0.212 mm (0.0083") thick. The autoclave cure parameters are defined by Cytec and are taken constant for all samples. The material properties available from the manufacturer are summarized as follows:

Fiber Tension	Strength	3013.01	(437)
	Modulus	155132.08	(22500)
Fiber Compression	Strength	1744.37	(253)
	Modulus	142721.51	(20700)
In-Plane shear	Strength	139.27	(20.2)
	Modulus	4826.33	(700)
Open Hole Compression	Strength	220.63	(32)
Fill Hole Tension (35 lb-in)	Strength	544.69	(79)
Open Hole Tension	Strength	-	-

Figure 17: CYCOM® 5276-1 Material properties[8], MPa *(Ksi)*

4.1.2   Tensile Test

The tensile test quantifies the axial strain, stress and modulus in the pulling direction. The interaction between this mechanical test and the mechanical properties is shown in the strain-stress relationship for an on-axis configuration (Equation 4):

$$\begin{Bmatrix} \varepsilon_1 \\ \varepsilon_2 \\ \gamma_{12} \end{Bmatrix} = \begin{bmatrix} S_{11} & S_{12} & 0 \\ S_{12} & S_{22} & 0 \\ 0 & 0 & S_{66} \end{bmatrix} \cdot \begin{Bmatrix} \sigma_1 \\ \sigma_2 \\ \tau_{12} \end{Bmatrix} \quad \text{where:} \quad \begin{aligned} S_{11} &= \frac{1}{E_1} \\ S_{12} &= \frac{-v_{12}}{E_1} = \frac{-v_{21}}{E_2} \\ S_{22} &= \frac{1}{E_2} \\ S_{66} &= \frac{1}{G_{12}} \end{aligned} \qquad \textit{Equation 4}$$

During the axial loading in the 1-direction, the axial stress (σ_1) is obtained from the testing machine data acquisition, which is the loading force divided by the cross-section area ($\sigma_1 = F_1/Area$). For this unidirectional loading, the term ε_2 and γ_{12} are equal to zero because the transverse directions are unconstrained. Then, the strain (ε_1) can be calculated using an extensometer or strain gages, which gives the axial modulus (E_1) and the Poisson's ratio (v_{12})[1]. Also, this technique can be applied at both the lamina and laminate levels. At the lamina level, all plies are in the same orientation and the modulus found is equal for all

---

[8] © 2009 Cytec Industries Inc. All Rights Reserved. *www.cytec.com*

28

plies. However, at the laminate level, the modulus depends on the entire laminate configuration and the properties are mainly used to predict the failure of this particular laminate. Therefore, companies need to investigate both lamina and laminate in order to validate, certify and predict the failure of their structures at each individual level. To determine these properties, a specimen is placed inside a testing frame that grips and applies a tensile force (created by shear loading) on its ends. this test is governed by the ASTM 3039 Standard[16], which gives the specimen geometries, the laminate configuration, the test procedure and the data acquisition method. The Figure 18 shows the setup and the real dimensions for the tensile specimen used.

$[0_4]_S$

$L_1 = 250 \; mm$

$L_2 = 76 \; mm$

$W = 25,4 \; mm$

$T = 7,91 \; mm$

$\Phi = 7°$

$t = 1,91 \; mm$

Glass Fiber Tab
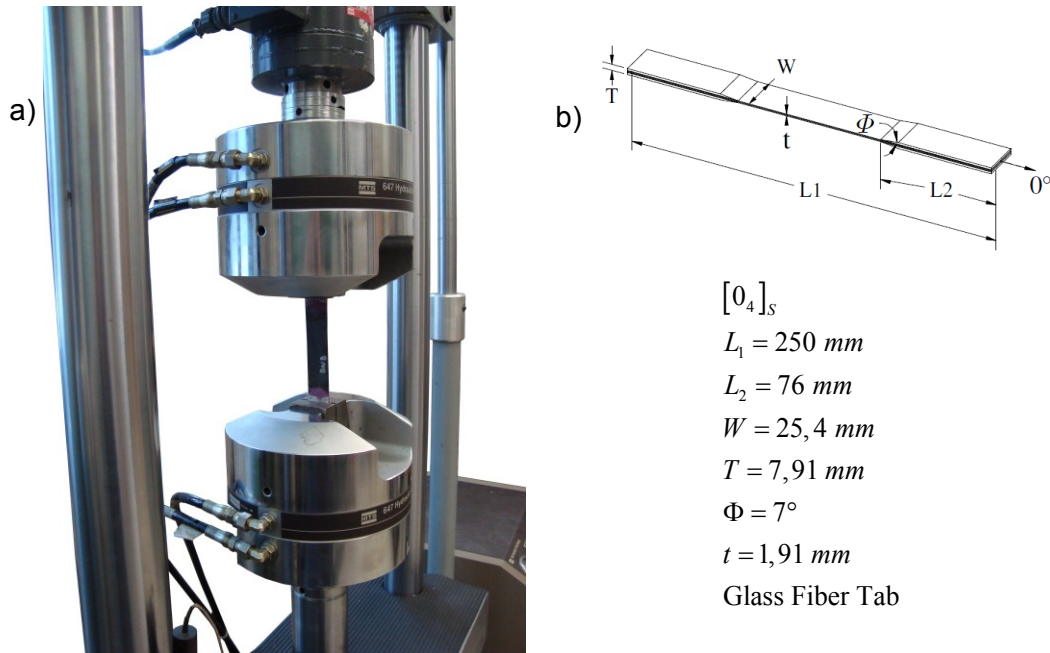
Figure 18: Tensile Test; a) Setup b) Sample geometries

In Figure 18b, the middle section represents the test (or gage) section and it is at this test section that the stress must be uniformly distributed. The laminate used for this test consists of eight 0° layers (in the pulling direction); therefore, the properties will be at the lamina level. The length is kept as long as possible to obtain a better stress distribution and to statistically produce repeatable results. The machine uses hydraulic grips to transfer the force between the testing machine and the specimen, which can damage the laminate at the contact surfaces. Therefore, E-Glass bonded tabs ($[0/90]_{7s}$) are added to protect the carbon fiber laminate from splitting by damaging the softer tabs during the load

transfer. Also, a taper situated at one tab extremity (see Figure 18) reduces the peel stresses created by the glue and, consequently, reduces the stress concentration at the beginning of the gage section and reduces the possibilities of tab failure. The test is executed by gradually increasing the load and recording the data until the specimen breaks. The ultimate strength of the laminate is the maximum stress that the specimen can carry. This investigation uses an extensometer in the gauge section to measure the deformation of the laminate during the entire test period and, consequently, the laminate modulus (slope of the stress-strain curve).

4.1.3   Compression Test

The compression test is somewhat similar to the tensile test in term of strain-stress relationship (Equation 4) because the only change is the loading direction (negative for compression). For composite materials, the tensile and compressive properties are not always the same, as opposed to a ductile metal, and for this reason two distinct tests need to be executed. Even if the strain-stress relationship is the same, the tests procedure is different and is governed by the ASTM 3410 standard [17]. The main specimen characteristic is a small gage length, which prevents buckling during the test. Buckling is an instability phenomenon and is the main problem with this kind of test; attention is needed to carefully design the specimen and align it properly during the test. Figure 19 shows the setup and the real dimensions for the compression specimen used.
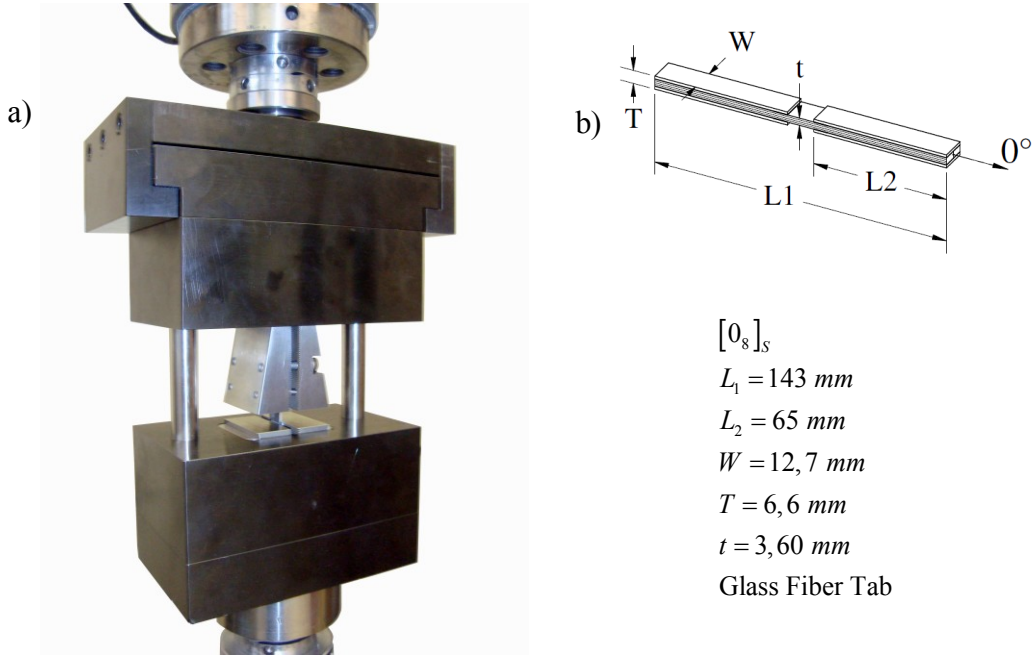
a)

b)

$[0_8]_S$
$L_1 = 143\ mm$
$L_2 = 65\ mm$
$W = 12,7\ mm$
$T = 6,6\ mm$
$t = 3,60\ mm$
Glass Fiber Tab

Figure 19: Compressive Test; a) Setup b) Sample geometries

To properly align the specimen during the test and avoid bending, buckling and twisting, the ASTM standard suggests the use of the IITRI fixture, which is used throughout this research. The fixture grips the specimen ends and applies a compressive force to create a uniform stress distribution in the gage length. Figure 20 shows the test fixture used for this study. The small gage length of these specimens must not only avoid the buckling effect, but also should help to obtain a pure compression failure mode. The laminate is prepared using sixteen unidirectional layers (along the compressive force direction). For the same reasons as in the tension test, tabs are bonded to protect the laminate from the machine grips (very penetrating grip feature). In order to avoid buckling, the test section must be small, the tabs must have flat ends (no tapers) and the fixture should be flush to the test section limits. For this test, the strength is found, similar to the tensile test. However, the strain is more difficult to record due to the small gage length, i.e. the extensometers cannot be used and the strain gages need careful manipulation. Strain gages need to be glued on the gage section according the standard and, with the help of a Wheatstone bridge, the strain can be read during the entire test. Also, two back-to-back strain gages quantify and discriminate the bending of the test section during the test. The introduction of a defect will create a small out-of-plane bending which is part of the influence of the

31

defect. This bending effect is approximated as small, consequently, it will not be considered during this study and only the strength will be recorded, which will by default include the bending effect of the defect. Furthermore, the compressive modulus is widely approximated as equal to the tensile modulus; in other words, the stress-strain slope between tension and compression values does not significantly change; only the strength varies.
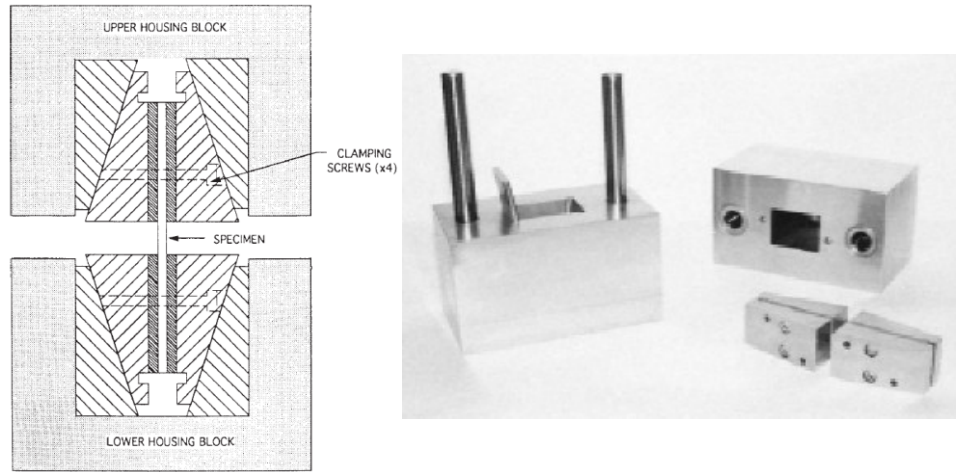
Figure 20: Compressive Test Fixture (IITRI Fixture) [17]

4.1.4   In-Plane Shear Test

The in-plane shear properties are the most difficult to determine because the stress field is not linear. For a square element, a pure shear loading must be applied on the four edges and the deformation must result in a diamond shape. In terms of strain-stress relationship (Equation 4), the in-plane shear stress is represented by the term τ_{12} and the strain by γ_{12}. These two parameters found by the instrumentation during the shear test (load cell and strain gages respectively), give the shear modulus (G_{12}) [1]. The shear test is complex to execute and requires a special fixture to apply the loading properly. Many in-plane shear test fixtures are available, but during this analysis the V-Notched Beam Method or Iosipescu (ASTM 5379 [18]) will be used due to its simplicity and the small size required for the specimens. In general, this test gives accurate results without extra care. Figure 21 shows the setup and the specimen dimensions for the V-Notched in-plane shear specimen.

a)

b)

$[0/90]_{4S}$

$A = 76\ mm$

$B = 20\ mm$

$C = 12\ mm$

$t = 3,60\ mm$
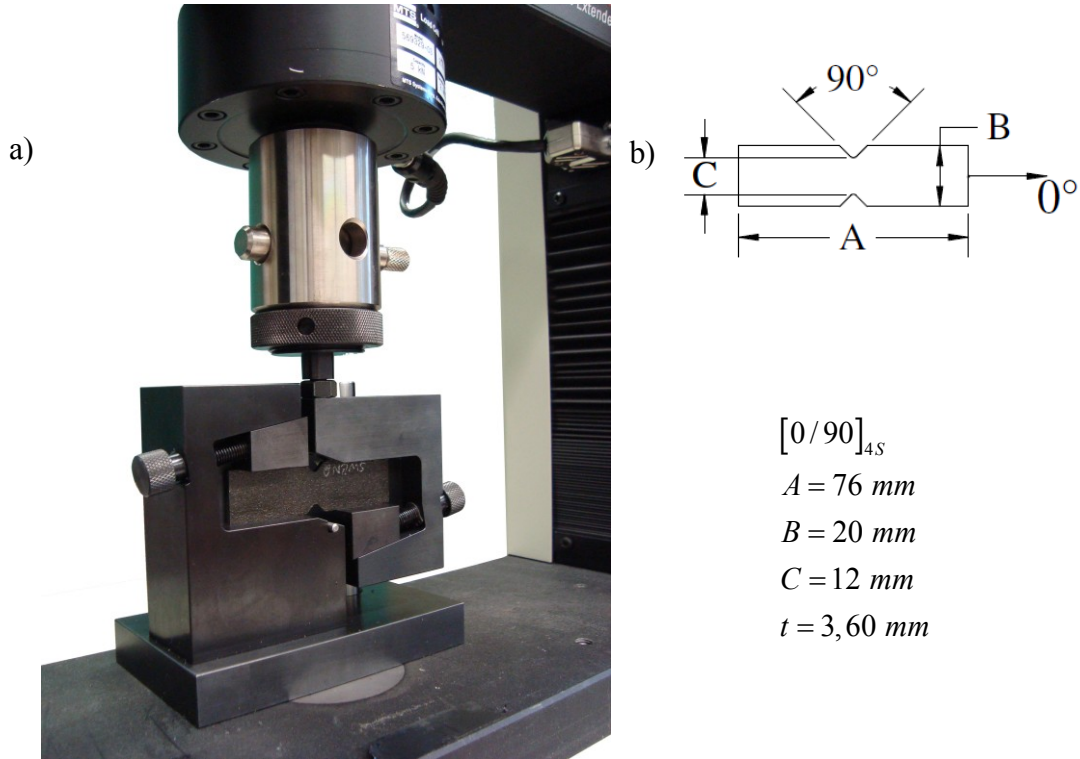
Figure 21: Shear Test; a) Setup b) Sample geometries

As shown in the above figure, the specimen consists of sixteen symmetric 0° and 90° plies, which is defined by the standard to obtain a pure shear stress state. The specimen has two "V-notched" shapes that act as stress concentrators to ensure that the failure occurs in the gage section (situated between the notches).

The fixture is created to allow the right side of the specimen to move while the other is kept fixed (Figure 22). The shear stress is created between the notches by applying a compressive load on the side that can move. During the test, the strain is recorded with the help of two strain gages at ±45° along the 0° axis or with a special Iosipescu shear gage between the V-notches. The Iosipescu Shear gage is more accurate than the two strain gage

Figure 22: V-Notched Beam Test Fixture Front View [18]

configuration because it can record the strain average on the entire gage surface and it has less variability depending on the position. The information from the strain gages gives the entire stress-strain curve of the specimen and, consequently, the in-plane shear modulus. Because of the non-uniformity of the strain field, the modulus is not taken into account and only the strength is recorded.
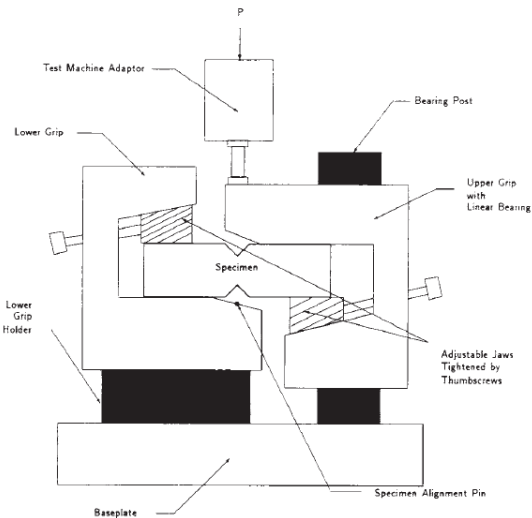
4.1.5 Open Hole Tension

The goal of performing an Open Hole Tension (OHT) test is to examine the reaction of a particular laminate with a stress concentration. The hole increases the stress around it and reduces the total strength of the laminate. This test is governed by the ASTM 5766 standard [19], which recommends the required dimensions and execution methods. To avoid the edge effect during the test, a width to hole diameter ratio (W/D) of at least six is suggested by the standard and considered in this experiment. This test method is used at the laminate level and the mechanical properties depend on the ply sequence of the laminate. In this study, the ply sequence has been defined by the standard and kept constant. When the specimen is loaded the stress and strain field around the hole change non-linearly, consequently, the strain and the modulus can only be found locally and are not representative of the entire structure. Moreover, since this test looks at the ultimate strength reduction of a statically loaded laminate, the modulus will not be taken into account during the investigation. Finally, Figure 23 shows the setup and the real dimensions for the OHT specimen used. For a quasi-isotropic laminate, tabs are not required during the test because the laminate is strong enough to avoid grip splitting. However, tabs have been optionally glued on specimens for precaution, but without real need.

$$\left[(45/0/-45/90)_2\right]_S$$
$$L_1 = 300 \; mm$$
$$L_2 = 76 \; mm$$
$$W = 36 \; mm$$
$$D = 6 \; mm$$
$$\Phi = 7°$$
$$t = 3,60 \; mm$$
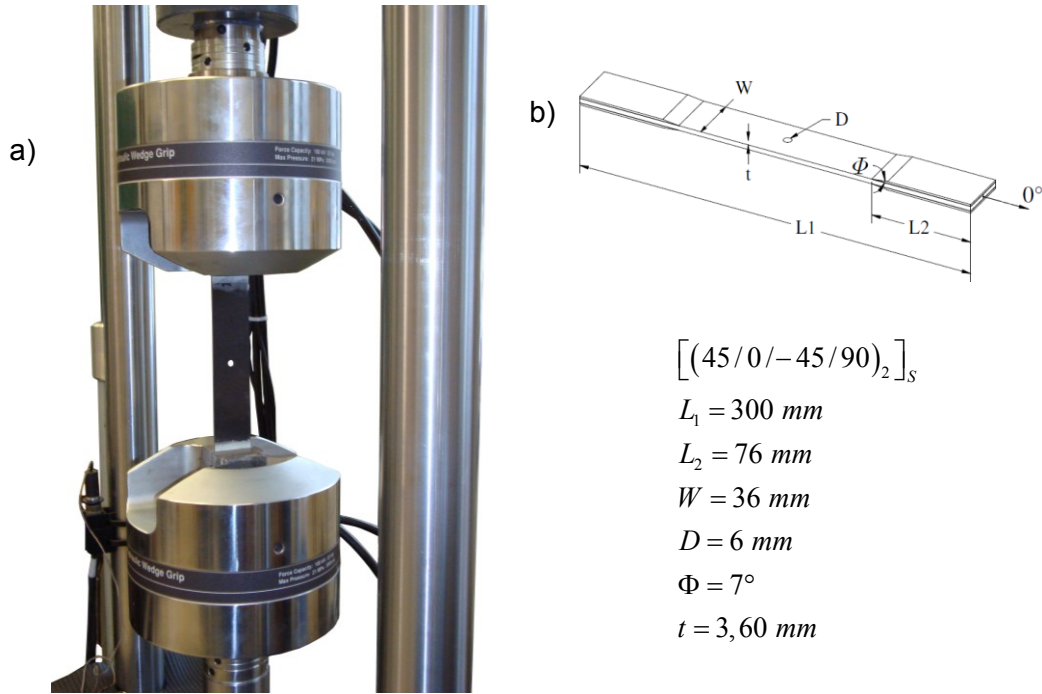
Figure 23: Open Hole Tensile Test; a) Setup b) Sample geometries

4.1.6   Open Hole Compression

The Open Hole Compression (OHC) executed for the same reasons as the OHT reveals the reduction of the ultimate strength in compression. The Open Hole Compression test geometry, execution and apparatus are governed by the ASTM 6484 standard [20]. Figure 24 shows the setup and the real dimensions for the OHC specimen used.

Like OHT, this test is performed using a quasi-isotropic laminate, which is defined by the standard and is different from the OHT test. The fixture (Boeing Open Hole Compression) constrains the laminate during the test in order to prevent the buckling of the laminate. The fixture is defined by the ASTM standard and is shown in the Figure 25.

a)

b)

$$\left[\left(45/-45/90/0\right)_2\right]_S$$

$A = 300 \ mm$

$B = 36 \ mm$

$D = 6 \ mm$

$t = 3,60 \ mm$
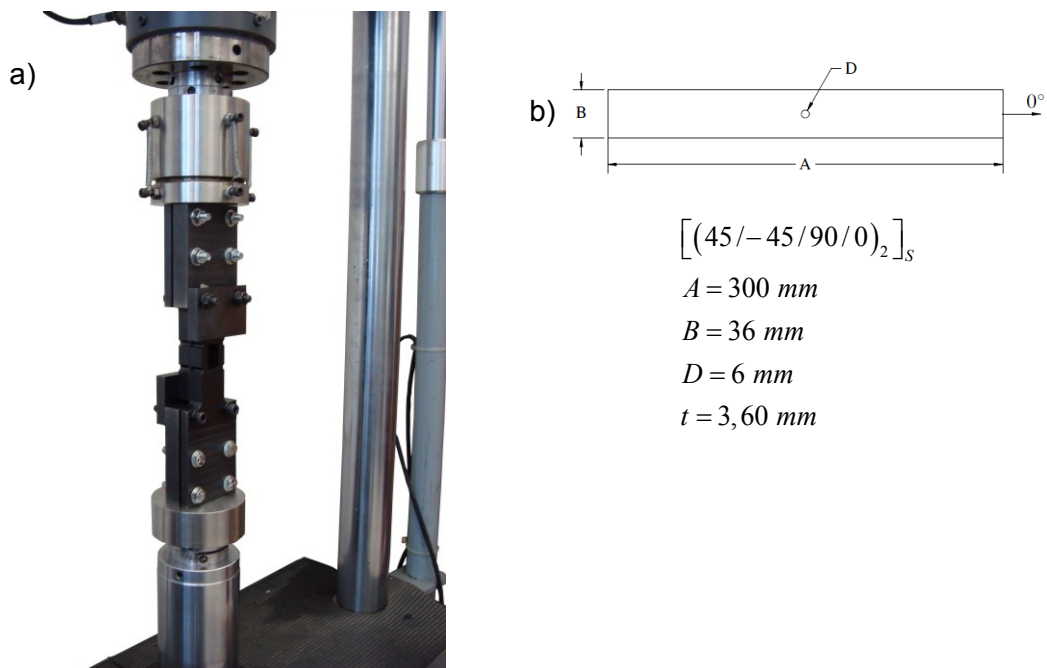
Figure 24: Open Hole Compressive Test; a) Setup b) Sample geometries

SUPPORT PLATE
(2 PLACES)

a)

STEEL SHIM
(AS REQUIRED)

GRIP AREA
(2 PLACES)

SPECIMEN

STEEL SHIM
(AS REQUIRED)

LONG GRIP
(2 PLACES)

SHORT GRIP
(2 PLACES)

b)

6 INCHES
WYOMING TEST FIXTURES, INC.
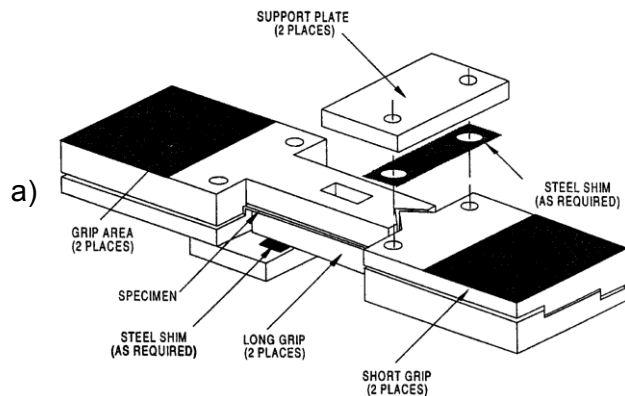
Figure 25: Open Hole Compressive Test Fixture (a) Isometric View[20] (b) Isometric Picture[9]

4.1.7 Micrograph Analysis

The micrographs look at the structure of the laminate to determine the crack growth, the failure mechanism, the overall configuration and structure of a laminate. To obtain a real portrait of the defect, coupons are cut, polished and photographed to see its tow configuration and geometry. This gives an idea about the real internal geometry after cure. Each defect configuration is observed and analysed to give complementary explanations about the failure mechanism. All micrograph results will be shown in section 5.2 for each experiment. Both, theoretical and real geometries will be compared to give information for future numerical analysis prediction of the defects. Moreover, a correlation will be made between the test results and the defect geometry to understand the influences on the failure mechanism. To complete the failure analysis, fractures for each type of defect are carefully observed (microscopy) to find a pattern between the failure mechanism and the defect.

CHAPTER 5: First Set of Experiments

The understanding of the failure mechanism and the impact of one basic defect is an essential step before analyzing the interactions of different defects' parameters. This section focuses on one gap, one overlap, one half gap/overlap and one twisted tow configurations, which are then compared with a baseline configuration (no defect). In this chapter, the details of the defect configurations will be explained, followed by a discussion of the results.

5.1   Details of the defect configurations

To be consistent with classical laminate theory and to keep the laminate symmetric and balanced, the defect is placed in the middle of the layers. Since the material used in the AFP process is usually thin and tough, it is assumed that one tow defect will generate a small effect. To increase its effect and to be able to capture the variability between configurations, the two middle layers are manually modified during the manufacturing in order to increase the defect area. Thus, the defect is placed in the middle layers of the laminate and centered within the coupons to reduce the bending effect associated with the asymmetry, thus ensuring only defect-induced bending. Then, the defect is orientated according the middle layer's orientation with respect to the laminate layup. This defect direction is differently defined for each test in order to predict the worst case scenario. All configurations and defect orientations are explained in the following sections, where the impact of the defects will be compared with the baseline configuration that contains no defect. As a result of the manufacturing process variations (tow width and tow placement tolerance variations), all samples contain small undesirable gaps and/or overlaps that are not removable. All samples are statistically covered by these small imperfections. The impact of these imperfections is not taken into account during this analysis, but it ends up being included in the results and the coefficient of variation.

5.1.1   One gap configuration

The one gap configuration recreates the impact of a tow missing during the manufacturing process. To generate a tow gap, two tows were manually removed one on top of the other. Also, the symmetry of the laminate makes the definition

of both middle plies similar and, consequently, their edges are aligned. Figure 26 shows the cross-section of the laminate, the position of the removed tows and

Figure 26: One gap configuration

the symmetry axis. Moreover, the defect's shape is kept constant throughout the specimen width or length, and in all the different tests. Section 5.1.5 explains in more detail the position of the defect for each type of test.

5.1.2 One overlap configuration

The one overlap configuration looks at the effect of adding a tow during the manufacturing process. Manufacturing complex shapes induces more variations in the position of the bandwidths than for a flat surface, which is similar to locally shifting the bandwidth. For this reason, every gap at one bandwidth edge creates an overlap on the opposite edge. This phenomenon and the possibility to define the gaps/overlaps ratio in the cut-and-restart option bring the need to investigate the structural effect of an overlap. The one overlap configuration has the same definition that the one gap configuration, but with added tows instead of removed tows. Figure 27 shows the overlap position and the symmetry inside the layup.
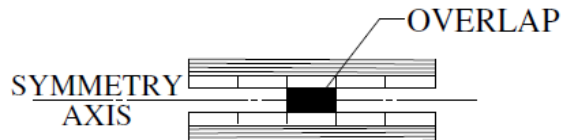
Figure 27: One overlap configuration

5.1.3 Half gap/overlap configuration

The percentage of gaps/overlaps at the bandwidth edges can be controlled by the process during the manufacturing (cut-and-restart option) in order to reduce gap area (resin rich) or overlap area (tow build up). This configuration should allow us to compare it with the one gap and the one overlap configuration and to see what kind of variation exists between them. This defect is created by

Figure 28: One half gap/overlap configuration

removing two tows, similarly to the one gap configuration, and by shifting them of

half a tow. The cross-section then consists of half a gap on one side and half an overlap on the other side, as shows in Figure 28.

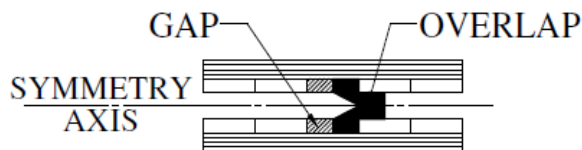### 5.1.4   Twisted tow configuration

A twisted tow is an undesire defect that appears when a tow flips upside down inside the guide and then is laid-down on the mould.
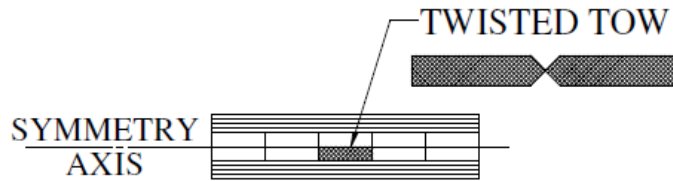

Figure 29: One twisted tow configuration

Usually an operator manually repairs this kind of defect because the real impact is misunderstood. Here, a twisted tow is manually created by modifying only one tow in one of the middle layers (Figure 29). Two reasons justify the use of one twisted tow in the laminate: i) it is difficult to perfectly align and place two twisted tows at the same location; ii) two twisted tows rarely appear close to each other. This defect configuration creates localized unsymmetrical laminate, which consists of two small triangles of resin rich area. However, these small sections do not affect the overall stiffness/bending matrix in the entire gage section. Furthermore, this configuration is not tested in both OHT and OHC because it is difficult to localize it, the precision and position of the drilled hole should influence the strength of the specimen.

5.1.5   Defect position in the coupons

As mentioned previously, the defect position depends on the estimated worst case scenario, which changes for the different tests. Tension and compression tests are executed to understand the impact at the lamina level, therefore, all layers' angles are kept at zero degrees along the loading axis. In other words, the defect is placed along the length, even if Sawicki and Minguet [10] have demonstrated for a compression test that a 90° defect induces more fiber waviness in the 0° layers and, consequently, increase the reduction of the mechanical properties. The position of the defect in shear coupons is much more difficult to predict and, for this reason, both 0° and 90° defect orientation is investigated. The open hole configuration induces a stress concentration that

locally increases the stress and induces an early failure. The stress around the hole changes for all locations and reaches a maximum at 90° about the loading axis. Consequently, the OHT configuration is investigated with the defect along the width. Also, the instability behaviour in compression, initiated by the fiber buckling effect, has questioned the real weakness of an open hole quasi-isotropic laminate. For this reason, the OHC test has its defect placed along the 0° axis to look at the impact of the defect combined with the buckling effect. However, more OHC samples are made with extra OHT laminates and, consequently, with the defects along the width in order to compare both defect orientations. Therefore, this last configuration has a slightly different layup than the OHC because of the different standards used to create the layup, but contains the same number of each ply angle, which allows capturing a trend between them. The impact of these changes to the layup is that the strength should be slightly different because it depends on the maximum angle between two consecutive plies, i.e. a higher angle provides a lower strength for the reason that it induces shear inside the laminate. For this reason, the strength cannot be compared between these two configurations but it can illustrate the overall defect impact compared with the baseline. All configurations are pictured in Figure 30. For each different test the defect position is represented by a thick line on the laminate and the arrow corresponds to the 0° axis.
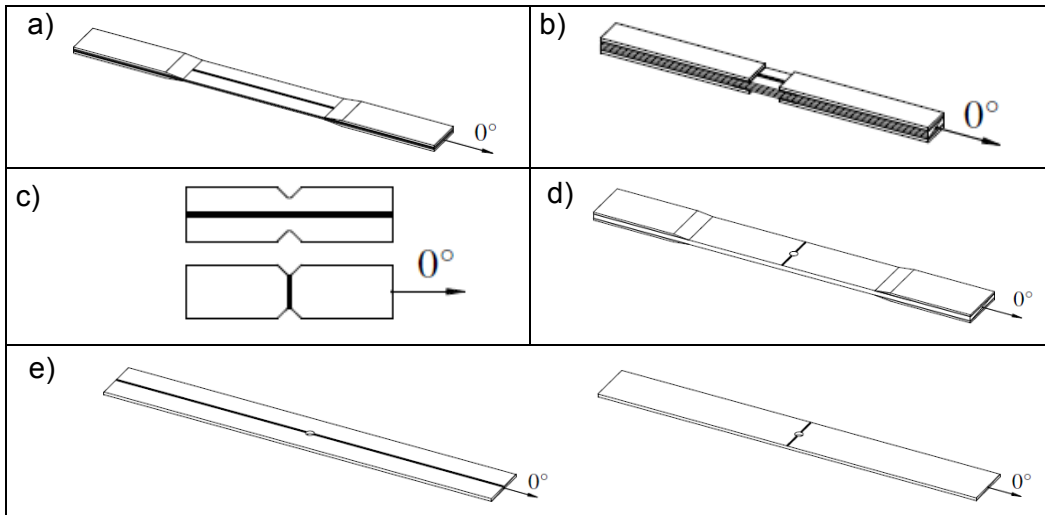

Figure 30: Defect position a) Tensile test b) Compressive test c) V-Notched shear test d) Open Hole tensile test e) Open Hole compressive test

5.2 Results and Analysis

After testing all configurations, graphs of the strength as a function of the test machine cross-head displacement have been plotted and compiled for all samples. The goal is to obtain the ultimate strength averages and the coefficients of variation for each type of defect. In addition, for each mechanical property, a bar chart sums up the defect effect to gain insight into the variations and the errors between samples. Failure analyses are carried out to understand the crack propagation behaviour and to correlate this behaviour with the strength results. Finally, for each test, the impact of the defect configurations is compared and the test sensitivity is quantified. Micrographs of all defect configurations are presented to understand the structure and evolution of the defects.

5.2.1 Micrographs analysis

The change in geometry and the effect of the tolerance related defects are difficult to predict and depend mostly on the layup. Micrographs of each defect configuration are presented in this section for each test to have a better understanding of the failure mechanism, the defect geometry, the thickness variation and the fiber waviness throughout the thickness.

5.2.1.1 Tensile specimens

The material and machine tolerances create random gaps and overlaps inside the entire structure that are situated along the tow edges. For the unidirectional layups, the staggering technique has been used to avoid the edge alignment through the thickness, to spread the defects more evenly and to obtain less thickness variations. Figure 32 illustrates a baseline configuration with the staggering technique used. As it is impossible to avoid tolerance-induced defects, it is interesting to see in Figure 31 that the tows
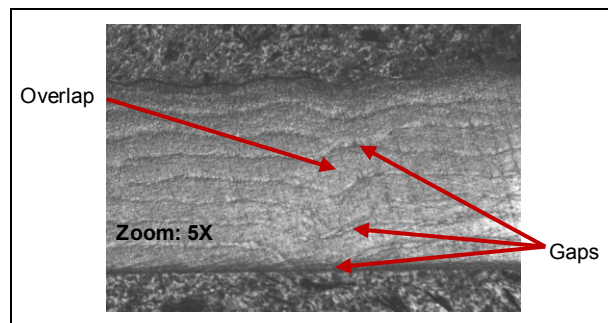

Figure 31: Random defects in a tensile baseline specimen (magnification 5X)

can move and sometime merge other tows in order to reduce the thickness variation.
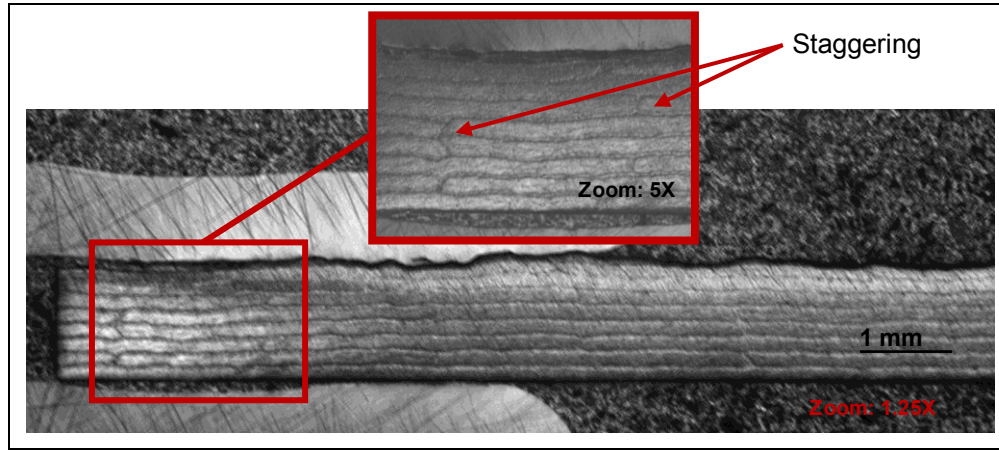

Figure 32: Tensile baseline specimen (magnification 1.25X and 5X)

Also, it can be seen for a unidirectional laminate that the gaps are not composed of resin rich areas because they are filled by other tows. The gap region in Figure 33 is filled by the other layers and the thickness variation is proportionnal to the two missing tows. In the same way, the
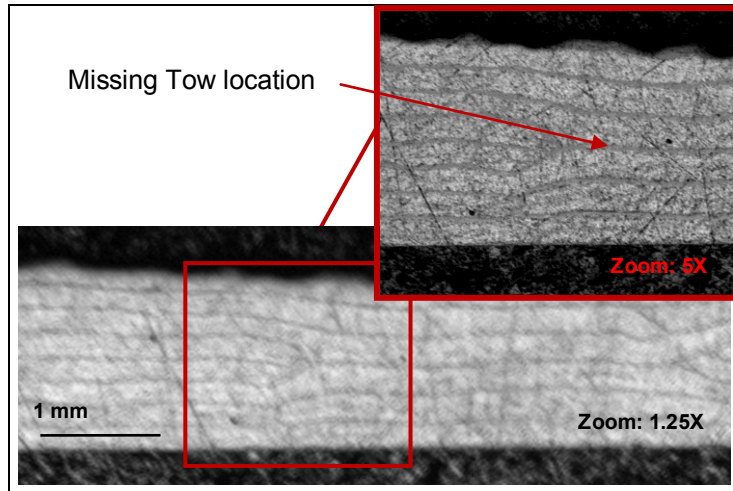
Figure 33: Tension gap specimen (magnification 1.25X and 5X)

thickness variation on the overlap configuration (Figure 34) seems to be of the same order of magnitude than the gap configuration. Again, the tows can move up to the junction of the discontinuity to prevent the formation of resin rich area. The half gap/overlap configuration is the best to illustrate the ability of adaptation in unidirectional laminate (Figure 35), which should represent the ability of each lamina. In this figure, all tows have adapted their shape during the cure process to fill the gap and to bypass the overlap. For a thin laminate, the high pressure of the autoclave increases the variation in the thickness of the laminate and the tow geometry (thickness and length) throughtout the entire sample. However, as the

thickness of the laminate increases the part is less sensitive to the variations (compare with 5.2.1.2 Compression pictures).
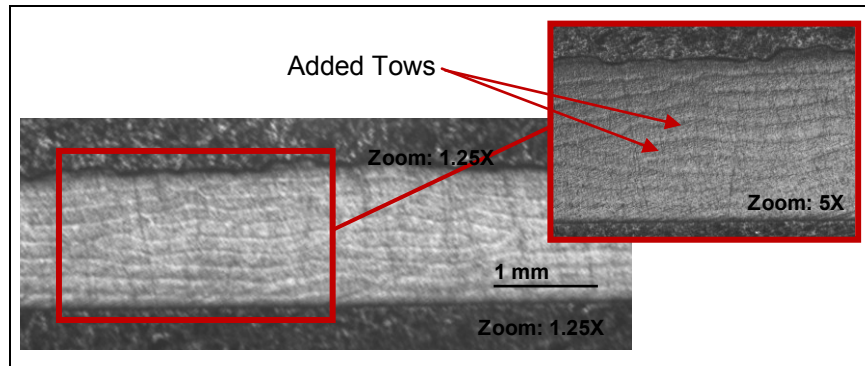
Figure 34: Tensile overlap specimen (magnification 1.25X and 5X)
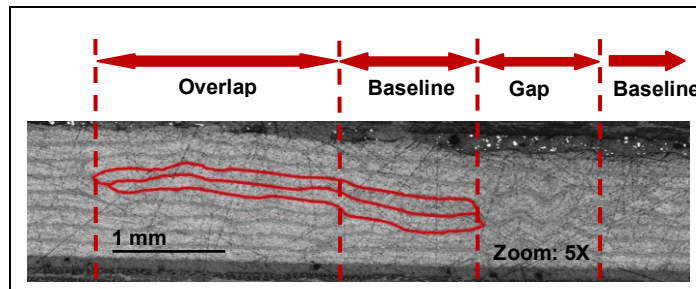
Figure 35: Tension half gap/overlap specimen
(magnification 5X)

5.2.1.2 Compression specimens

The fiber compression specimens are similar to the tension specimens but contain more plies. So, by increasing the number of plies, the laminate has more probability to end up with defects, one on top of the other. However, the previous effects and conclusions from the tension micrographs are still applicable for the compression laminate. The overall thickness variation is smaller than that of the previous test that contains fewer plies, since the added layers help to hold and distribute the pressure of the autoclave. Like the tension samples, the consolidation of all defect configurations is good, as shown in Figure 36 for the baseline, Figure 37 for the gap, Figure 38 for the overlap and Figure 39 for the half gap/overlap configuration.

Figure 36: Compression baseline with random defects specimen (magnification 1.25X and 10X)

Figure 37: Compression Gap specimen (magnification 1.25X)

Figure 38: Compression overlap specimen (magnification 1.25X and 5X)
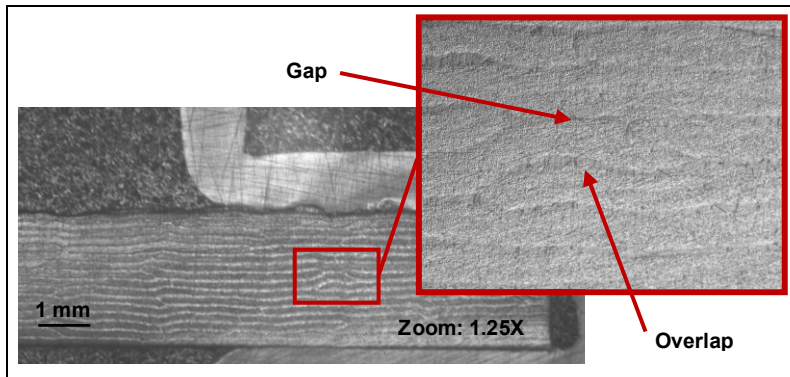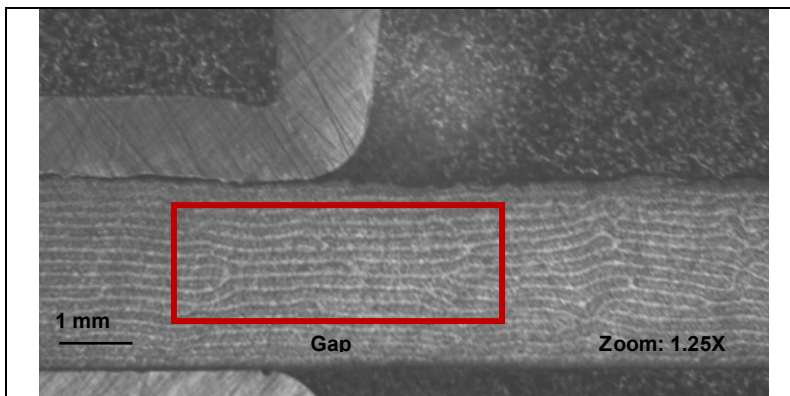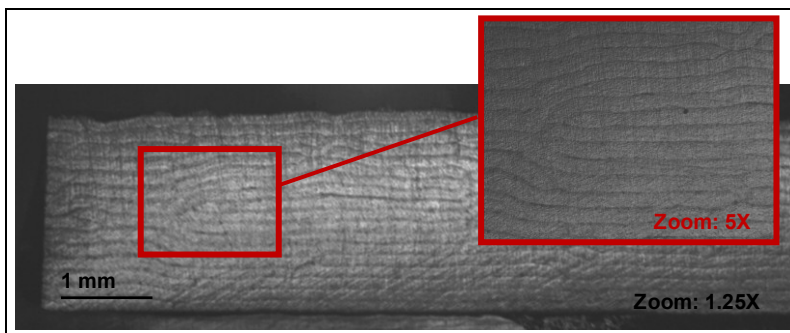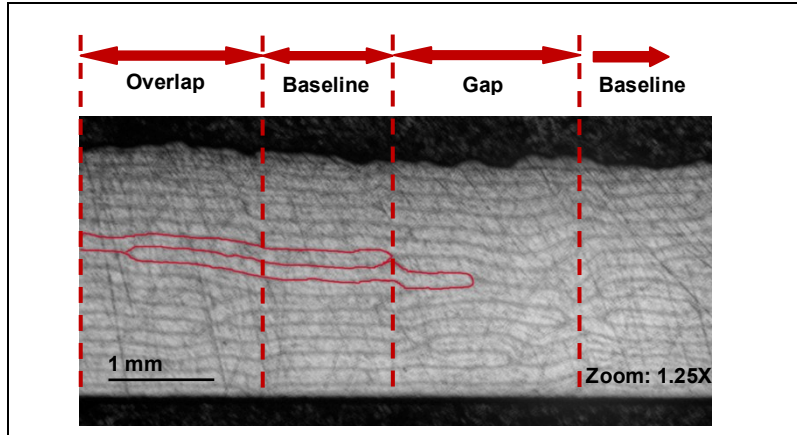
Figure 39: Compression half gap/overlap specimen (magnification 1.25X and 5X)

5.2.1.3 In-Plane Shear specimens

The in-plane shear specimens have a different layup that the previous tests (0°-90°) and, consequently, the overall internal geometry is different. The defect geometry and consolidation in the middle layers are similar to the previous unidirectional configurations. However, the other plies need to self-adapt and curve themselves as a function of the middle layer thickness. As seen previously, tows with the same orientation can easily move and merge, but the new 90° plies need to bend, along its fiber orientation, according to the thickness variation. So, the defect size is a critical parameter, especially when loaded in compression, because smaller the defect is, smaller the radius of curvature will be. Nevertheless the introduction of 90° layers add complexity to the defect geometry, it also increases the out-of-plane stiffness of the laminate. Consequently, it takes more pressure during the cure process to bend all 90° layers and to fill a gap type of defect. This explains why the gap configuration usually is composed of a small resin rich area (Figure 40), which does not occur for unidirectional laminates. The constraint induced by the flat mould creates the out-of-plane fiber waviness only on the layers on top of a defect (vacuum bag side), and it is true for all defect configurations. In addition, the 90° layers create an uneven resistance throughout the thickness to the autoclave pressure and generate non-constant fiber waviness for each layer. This fact is true for all types of defect; the fiber waviness is higher if the fiber is close to the layer with the defect and it is smaller as it reaches the top layers. The overlap configuration

46

(Figure 41) has a better integrity and the fiber waviness is more throught the thickness than the gap configuration because all layers are self-suported.
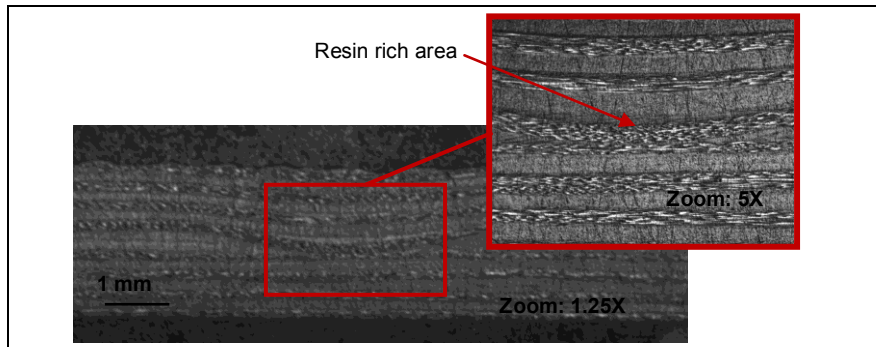
Figure 40: In-plane shear gap specimen (magnification 1.25X and 5X)
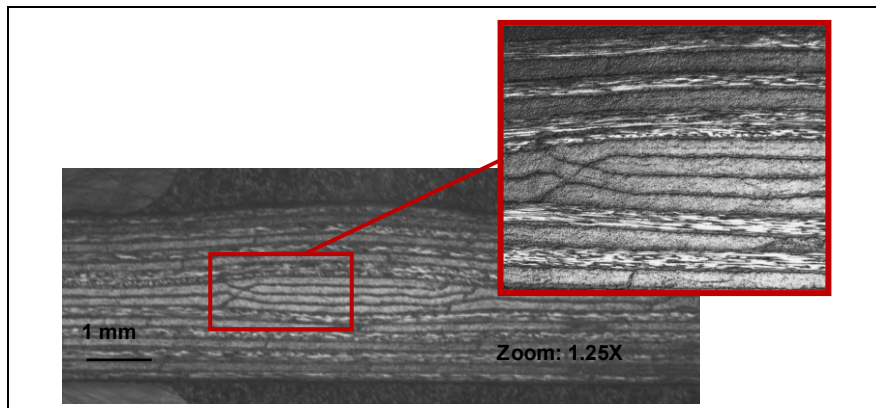
Figure 41:In-plane shear overlap specimen (magnification 1.25X and 5X)

The half gap/overlap configuration (Figure 42) is guided by the same rules as the two separete defects alone but at a smaller scale. For this configuration the gap size is two times smaller, thereby increasing the fiber waviness effect (smaller radius of curvature) as well, increasing the resin rich area. However, the fiber waviness in the overlap section is similar to the full overlap configuration. This shows that the overlap does not seem to be affected by its size, as opposed to the gap configuration.
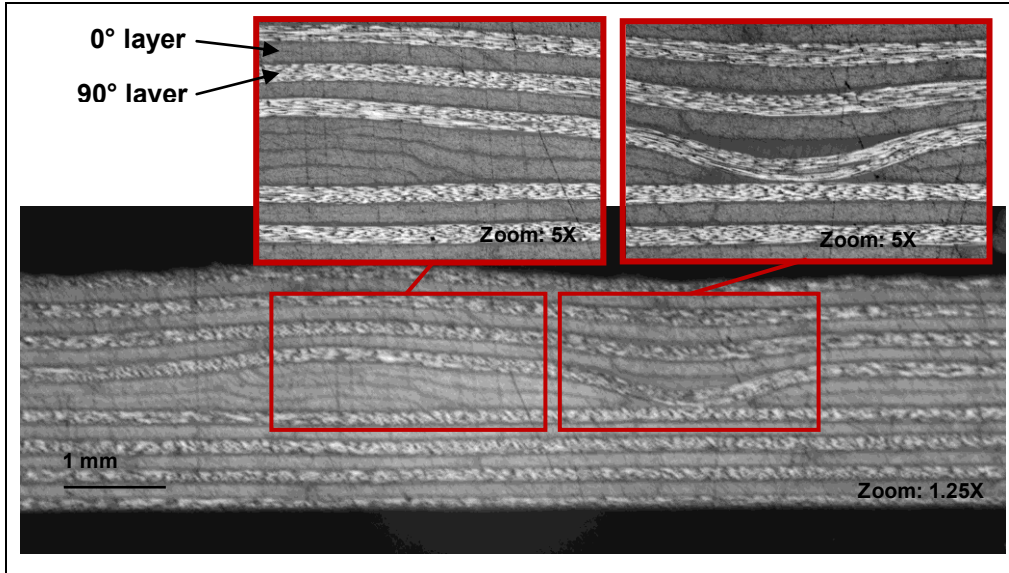
Figure 42: Shear half gap/overlap specimen (magnification 1.25X and 5X)

5.2.1.4 OHT and OHC specimens

The OHT and the OHC laminate are similar in terms of geometry (Figure 43) and the small difference of the stacking sequence does not influence the defect and the overall geometry. For this reason, they were combined and analyzed in the same section. Figure 43 illustrates both baseline configurations. In this figure, the random defects of the OHT do not influence the overall thickness and do not create a large amount of fiber waviness because they are too small and the resistance through the thickness should be higher than the shear laminate. Consequently, all small gap areas are filled by resin. Also, the smaller fiber angle obtained between two consecutive plies in the OHT specimen helps each layer to self-adapt, to reduce the resin rich area and obtain a more uniform thickness.
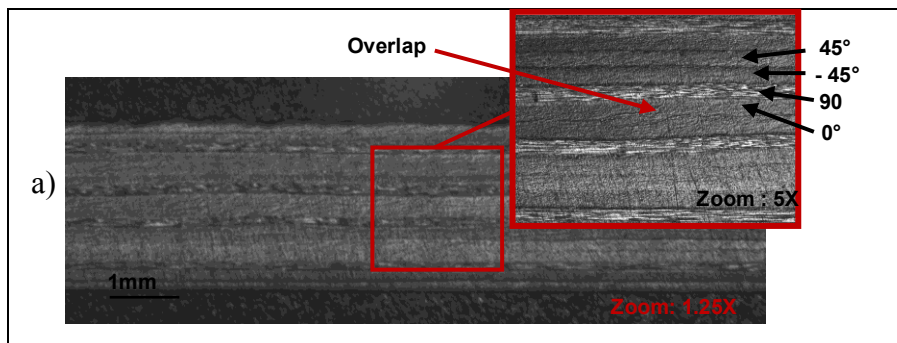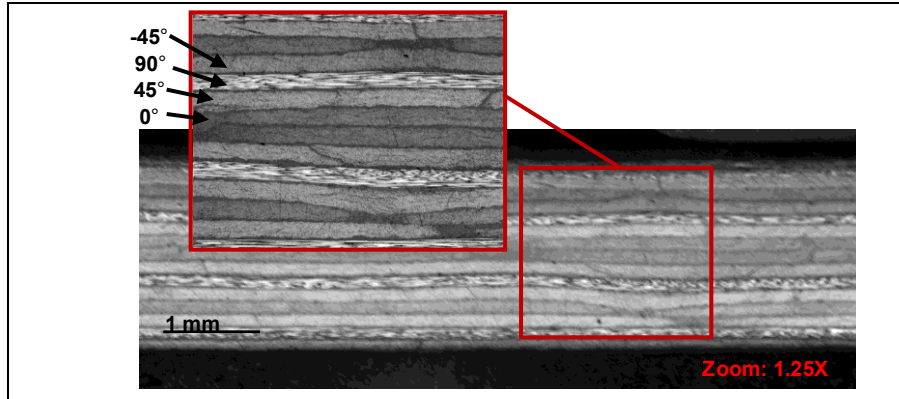
**Figure 43: a) OHC baseline specimen (magnification 1.25X and 5X);
b) OHT baseline specimen (magnification 1.25X and 5X)**

The gap configuration (Figure 44) and the overlap configuration (Figure 45) show similar geometries that were obtained during the in-plane shear test. These similarities mean that the difference in layup does not have significant effect on the integrity of the laminate when using full gap and overlap type of defects.
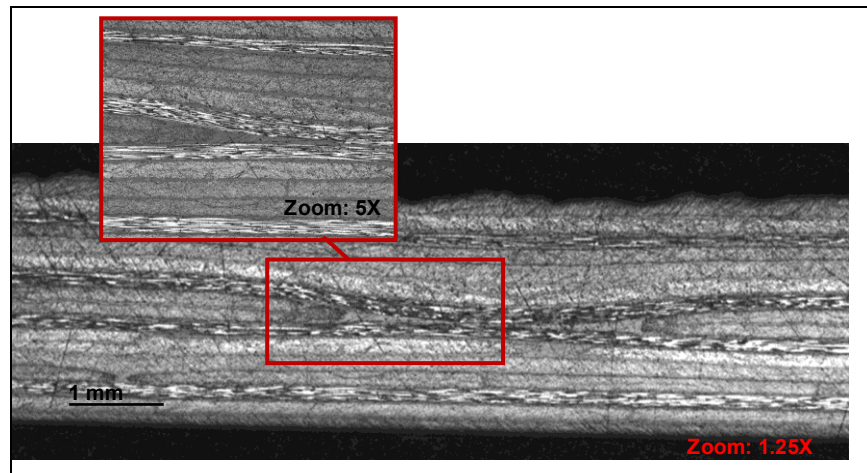
Figure 44: OHC gap specimen (magnification 1.25X and 5X)
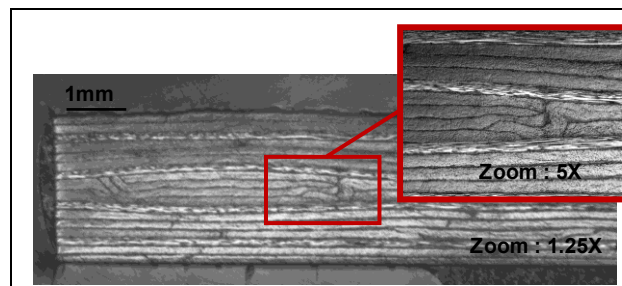
**Figure 45: OHC overlap specimen
(magnification 1.25X and 5X)**

49

As mentioned previously, a smaller angle between two consecutive layers helps to reduce the size of a resin rich area and can be seen in Figure 46 for a half gap/overlap configuration. Even with the high pressure of the autoclave, the resin rich area rarely contains voids as represented by the black spot on the OHT specimen (Figure 46b).
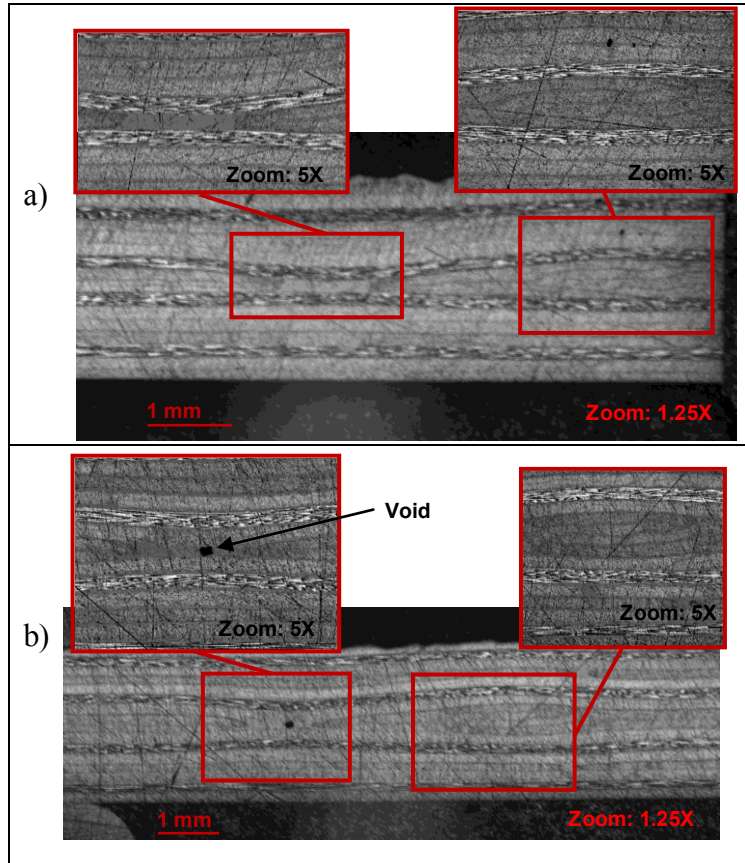
Figure 46: a) OHC half gap/overlap specimen; b) OHT half gap/overlap specimen; (magnification 1.25X and 5X)

5.2.2 Tensile Test

All tensile tests failed in the middle of the gage section and demonstrated a catastrophic failure, which is a multi-mode mode of failure (mix of explosive, lateral, angle and longitudinal splitting) and is characteristic of a high toughness material. A catastrophic failure is the consequence of a good load distribution inside the gage section, in other words, the tabs efficiently transfer the load to the fibers and the failure occurs suddenly in the entire test section. Figure 47 shows a typical fracture for a coupon without defect.

Figure 47: Typical Tensile fracture for a coupons without defect

In addition, the type of fracture agrees with the Stress-Displacement curve, which is shown in Figure 48 for a typical coupon without defect. As the specimen is loaded the stress linearly increases, up to its limit, and then breaks apart. Also, as expected, this curve shows almost a constant modulus (slope of the stress-strain curve) along the entire test. This graph gives a good overall idea of the modulus' shape because its slope looks very similar to the real stress-strain curve. However, the modulus cannot be found form the strain/head-displacement curve because the specimen can slip inside the grips. On the other hand, the ultimate strength, which does not change between stress-strain and stress-displacement curves, represents the highest stress that the specimen can carry. Figure 50 compares together the impact of the defect configurations on the ultimate strength. In this figure, the average values of the specimens and the error bar in term of the coefficient of variation are illustrated for each defect configuration.

Figure 50 shows that the impacts of the defect are small with a maximum of 4% decrease for the half gap/overlap, and 3% increase for the twisted tow configuration. Even if the effects are small, trends are noticed between the configurations. The broken half gap/overlap specimens make

Figure 48: Stress-Displacement relationship for a tensile coupon without defect

clear the reason why this configuration has seen the biggest decrease of its ultimate strength. During the loading the defect tends to become straight and,

51

consequently, creates an out-of-plane force (Figure 49) that initiates the early failure. Furthermore, the shifted tows of this defect are aligned with the tows of the upper and lower layers because the laminate was manufactured using the staggering technique. This alignement creates a weak region that is favorable for fiber splitting and crack propagation.

Figure 49: Half gap/overlap out-of-plane effect

The other negative impact is obtained by the gap configuration (2% reduction) compared with the baseline configuration. The failure seems to be driven and initiated by the lower stiffness region that is within the gap. On the other hand, the overlap configuration has shown a negligible improvement (1%) that seems to be driven by the addition of material which creates a stiffening effect. Rather than calculating the real and complex shaped cross-section area, an average has been used for each specimen and, consequently, can explain the small improvement. Finally, the twisted tow configuration shows an improvement (3%) that could be explained by its stress-strain field. However, to obtain confirmation and a better understanding of this mechanism, further investigation is required.
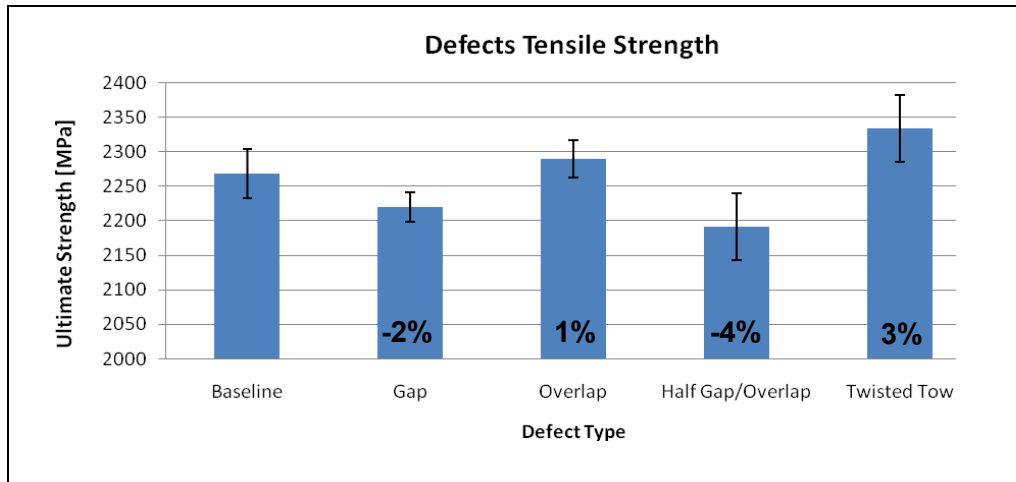
Figure 50: Tensile Strength variation as a function of the defect type

5.2.3   Compression Test

All compression specimens have failed according to the transverse shear or through-the-thickness modes of failure, which have been defined as acceptable modes of failure from the ASTM standard. Figure 51 shows a sample without defect that has broken with a brooming failure mode that demonstrates a perfect compressive failure.
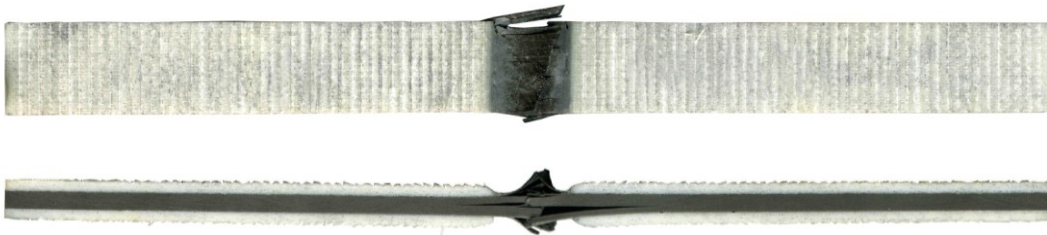
Figure 51: Typical Compression fracture for a coupons without defect

For each test, a Stress-Displacement curve was recorded and plotted, which is very similar to the tension test but with a lower strength. Figure 52 illustrates a typical relationship for the baseline configuration. At the beginning of the curve (from left to right) the wedge-grip features penetrate the fiber-glass tabs instead of loading it and, consequently, the stress rises at a low rate. After the wedge-grips feature has fully penetrated the tabs, the stress rate starts increase constantly and up to the final failure. This last increase indicates that the modulus is constant as predicted. However, as for the tension test, the modulus value

cannot be found from this curve and strain gages are needed to obtain its value. From all these curves, the ultimate strength is recorded as the highest stress before failure and compiled in order to obtain the comparison between the defect configurations (Figure 53).
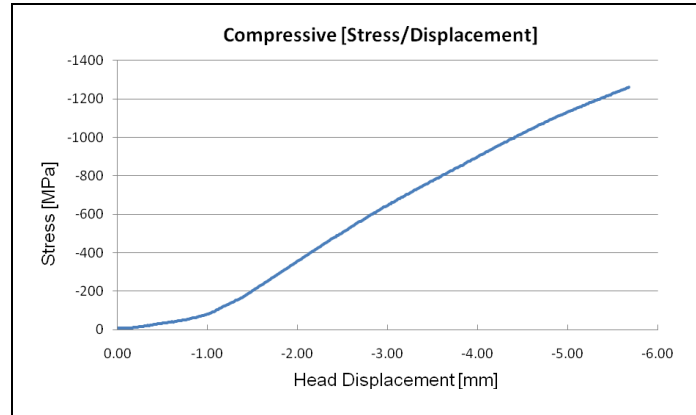
Figure 52: Stress-Displacement relationship for a compressive coupon without defect

Similar to the tension test, the small resulting variation demonstrates the small effect of the defects at the lamina level with a maximum of 1% decrease for the gap configuration, 7% increase for the overlap configuration and no changes for the other configurations. However, the high coefficient of variation for all these tests makes it difficult to classify the impact of the defects. The only possible conclusion is that the overlap configuration improves the overall strength because its coefficient of variation does not cross the other coefficients. So, the negligible effect of the defects at the lamina level lead to the same conclusion as that of Sawicki and Minguet [10]: the effect is more pronounced at the laminate level than the lamina level because, when the defect is placed at 90° of the load, micro-buckling is induced earlier.
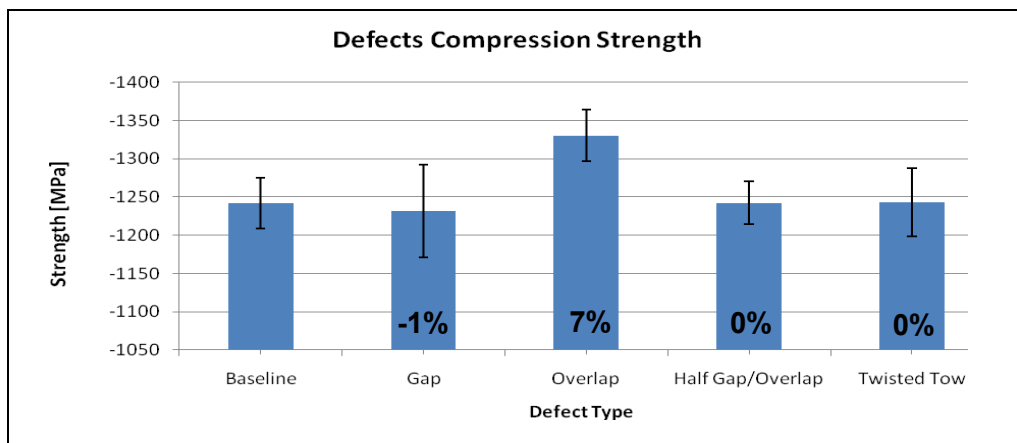
Figure 53: Compressive Strength variation as a function of the defect type

5.2.4   In-plane Shear Test

The failure of the V-Notched beam method is dependent on the layup used. In this case, a [0/90] layup gave a pure shear state between the notches and, consequently, influences the type of failure. All the in-plane shear samples have shown an acceptable failure, which is represented by the fibers shifting in the 0° layers and a matrix cracking in the 90° layers. All samples have shown a plastic deformation at the end of the test, which is characteristic of high toughness material. Figure 54 illustrates the typical failures for both defect orientations without defect. To create the different defect orientations, the layup has been rotated of 90°, which has not affected the shear properties and the fracture characteristics: defect along the length [90/0] and defect along the width [0/90°]. Consequently, on this figure, both samples have the same failure mechanism but the crack pattern on the top layer is more visible than the second layer, which explains the small difference between them.
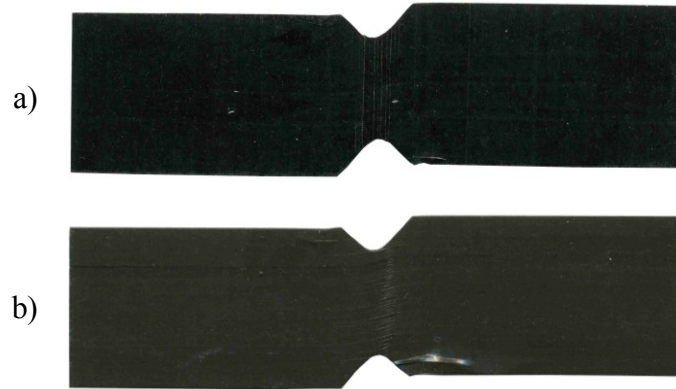
Figure 54: Typical V-Notched fracture for a coupon without defect; a) defect through the length; b) defect through the width

The typical stress-displacement curve is presented in Figure 55 for a baseline configuration. For the [0/90°] layups, the recorded curves are non-linear and are similar to the typical standard results. The curve shows two distincts moduli during the test, i.e. at the beginning the modulus is high and, almost at the middle of its ultimate strength, decreases and stays constant until the end. Moreover, for the 0-90° layups the ultimate strength is recorded as the highest value before the first drop in stress, which designates the first internal failure. After this drop, the sample carries more loads up to the final failure or the fixture limit. Most of the

samples have seen this first load drop but few of them have seen only the final failure, which is characteristic to tough material or thermoplastic resin system. For this particular behaviour, the ASTM 5379 standard suggests that the ultimate strength is equal to the stress at 5% strains. However, the absence of strain gages did not allow using this criterion directly. Consequently, all specimens with an overall reduction of less than 1 MPa have not been considered. Despite this last constraint, all specimens of the twisted tow configuration with the defect along the length have been ignored. Nevertheless, to obtain an idea of the strength for this configuration, a numerical analysis, with non-linear material properties based on tests, has linked the shear strain with the head displacement to give an idea of the ultimate strength. Considering that the analysis has presumably underestimated the properties (comparison with experiment), the real values should be higher than the values found with this numerical method. Even with the use of strain gage, the 5% criterion sometimes occurs during the plastic deformation and is not really relevant to evaluate the ultimate strength.
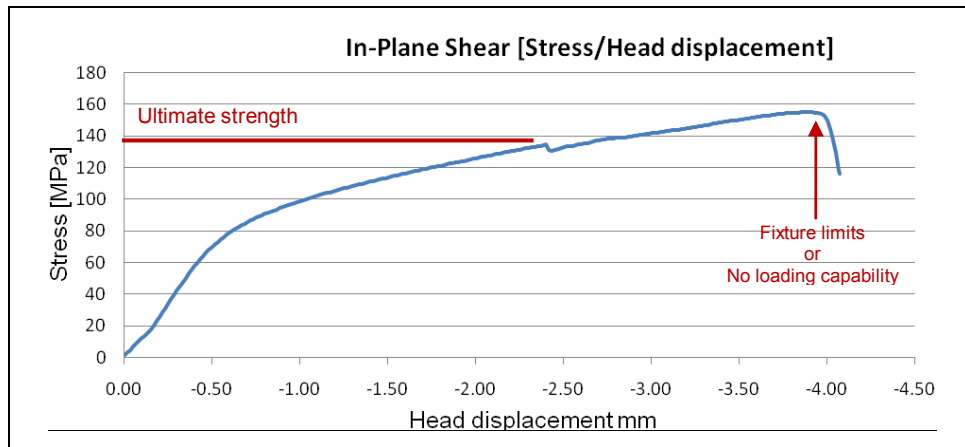
Figure 55: Stress-Displacement relationship for a In-plane Shear coupon without defect

All values are summarized on the bar chart in Figure 56 for the defect along the length and in Figure 57 for the defect along the width. A quick look at both figures indicates that the defect along the width causes more strength reduction than the defect along the length with a 12% maximum reduction compare to 8% maximum reduction respectively.

The configuration with the defect along the length shows a small effect on the ultimate strength with a maximum reduction of 8% for the half gap/overlap. The

ultimate strength does not seem to be affected by both gap and overlap with around 1% reduction. Here, the twisted tow configuration has been found using the 5% strain approximation as mentioned above and, again, the real strength should be higher. Consequently, this last configuration has negligible effects on the strength with less than 3% decrease.

On the other hand, the configuration with the defect along the width shows larger effects on the ultimate strength with 12% maximum reduction for the overlap and 3% maximum improvement for the gap configuration. For this last defect orientation, the failure mechanism seems to be guided by the fiber waviness in the 0° layers, i.e. the bigger the deflection of the waviness, the more the strength decrease. Therefore, the half gap/overlap configuration shows 5% decrease, which is directly proportional to both gap and overlap configuration. In this configuration, the deflection is smaller than the overlap configuration and bigger than the gap configuration, as observed in section 5.2.1. Again, the twisted tow does have a significant effect with its 3% decrease. Another overall conclusion for this test is that, even for one defect configuration, it is difficult to capture the effect of the defect because of the small test section but a good idea of the mechanisms can be obtained. So, for better verification, other tests should be tried on another fixture with a larger test section.
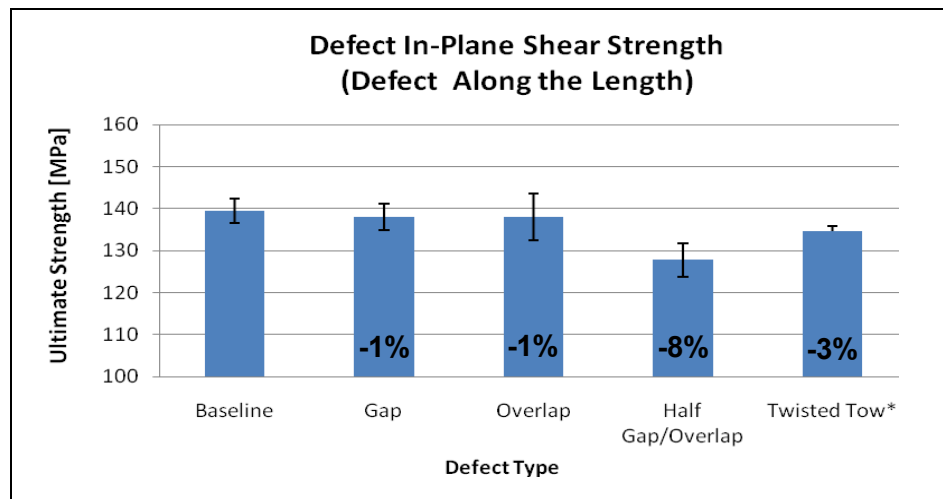
Figure 56: In-plane shear Strength variation as a function of the defect type along the length
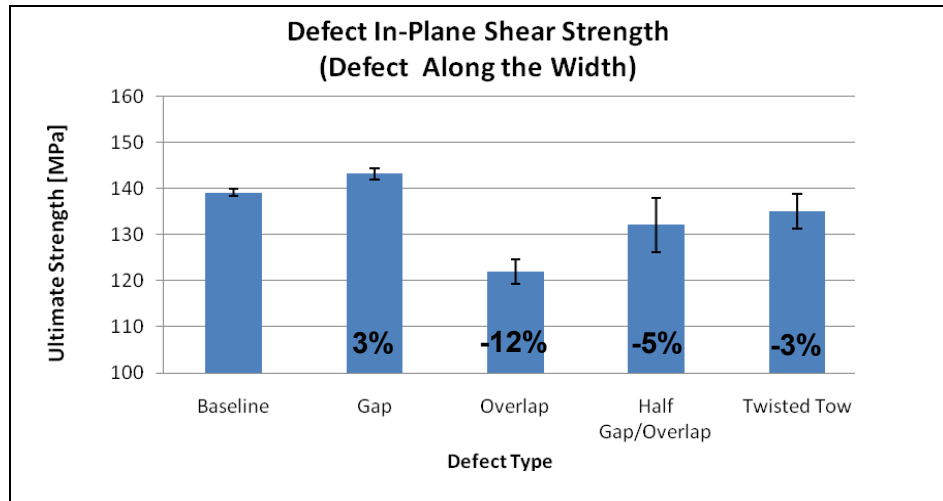
Figure 57: In-plane shear Strength variation as a function of the defect type along the width

5.2.5   Open Hole Tension

The Open Hole Tension ultimate strength is similar to that of fiber tension: the values are slightly lower. Typical OHT failure occurs in the weakest plies first, which are the 90° and the ±45° plies. This failure behaviour was observed throughout this study with usually one side of the hole breaking at 90° and the other at 45°. Also, the hole creates perturbations in the stress field all around it and, more specifically, it shows a maximum increase along the center and perpendicular to the load. Consequently, cracks are initiated at this position and propagate to reduce the ultimate strength. Figure 58 shows a classic failure that occurs for a coupon without defect.

Figure 58: Typical OHT fracture for a coupons without defect

Each sample result has been recorded and illustrated on a stress-displacement curve as shown in Figure 59 for a baseline configuration. This curve gives a good idea of the linear modulus behaviour for the first 95% of the strength. At the end of the test, the strength
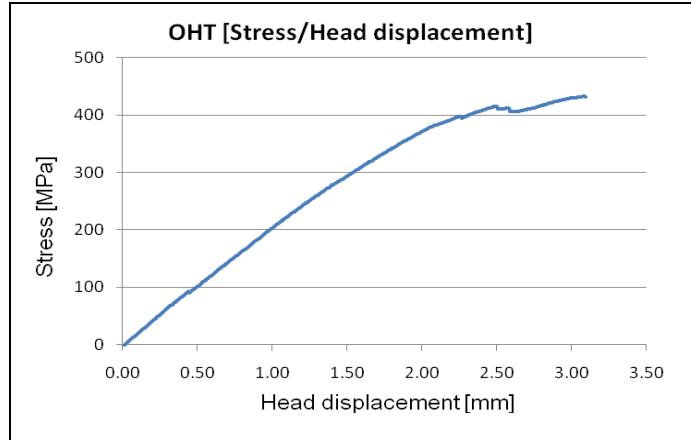
Figure 59: Stress-Displacement relationship for a OHT coupon without defect

shows sagged tooth behaviour, corresponding to the damage on layers, and up to the final failure. Similar to the tension test, the ultimate strength is the highest value of the stress that the specimen can carry (computed using the cross section without the hole). Figure 60 compares all the different defect configurations together.

As illustrated in the figure, no significant influence is observed between all these defects, with a maximum ultimate strength decrease of 1% for the gap configuration and a maximum improvement of 2% for the overlap configuration. The half gap/overlap configuration, on the other hand, results in properties that are in between both of them (1% improvement). During the loading, the addition of material of the overlap delays the crack initiation by adding a stiffener at the stress concentration area and, consequently, improves the property. Then, the overall effect of these defects in OHT is negligible and confirms that the stress concentration factor has more effect than the defect itself. This conclusion matches Turoski's experiment results [15], in which, for a similar toughened material it was suggested that a three-gap configuration has more impact in an unnotched tensile specimen (around 15%) than in a specimen with a 0.25 inch [6.35 mm] hole (less than 1%).
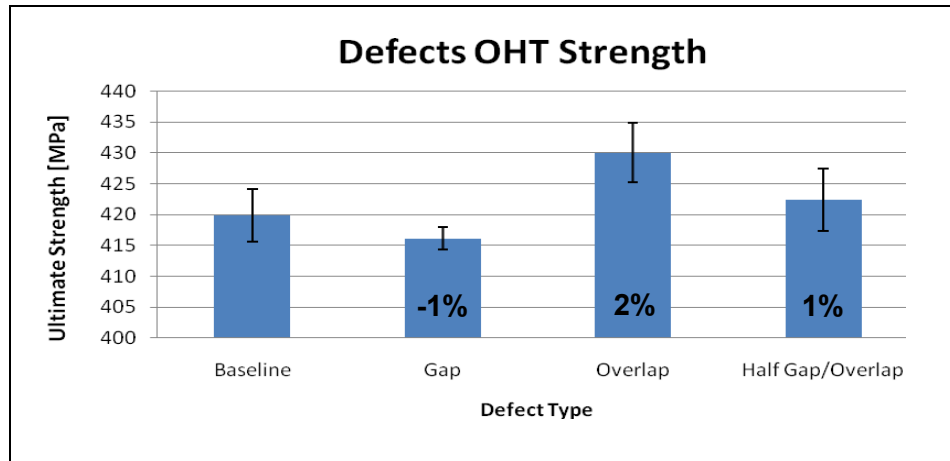
Figure 60: OHT Strength variation as a function of the defect

5.2.6 Open Hole Compression

All OHC samples have failed with the same typical toughened material behaviour. During the compression, the failure occurs first under the weakest layers, which are the 0° and the ±45°. Figure 61 shows a typical failure that has occurred on a baseline OHC specimen.
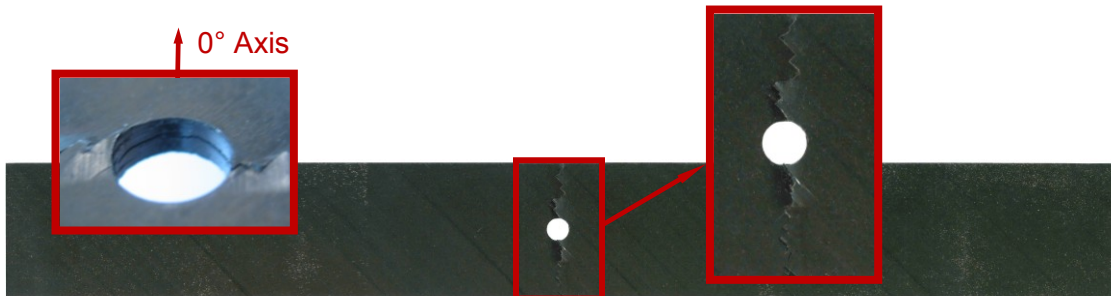
Figure 61: Typical OHC fracture for a coupon without defect

According to Suemasu et al.[21], this failure mechanism is unique to tough resin systems as it is characterized by a micro-buckling of the 0° plies at the area highest stress concentration. A delamination between the next layers follows and the cracks propagate within the interfaces. Finally, the propagation goes all around the hole circumference as illustrated in the last figure. This toughened mechanism determines the strength of the laminate, in other words, the bigger the delamination size, the higher is the strength. The OHC test combines with

tough materials can also allows determining the material performance according to damage tolerance.

For each sample the stress-displacement curve has been plotted as shown in Figure 62 for a typical baseline configuration. Each defect configuration is similar to the baseline configuration with the exception of the amplitude of the strength. Similar to the compression test, the OHC stress-displacement curve is characterized by a constant modulus and a sudden failure. In this figure, the small curvature of the curve can be explained by a small movement of the specimen inside the fixture. Like the previous tests, the ultimate strength is represented by the highest stress
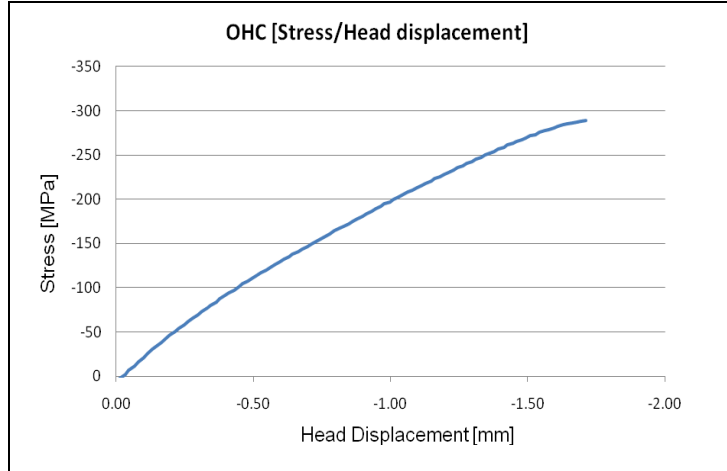
Figure 62: Stress-Displacement relationship for a OHC coupon without defect

before failure. With all these values, comparison charts have been constructed for both defect orientations (Figure 63 for the defect along the length and Figure 64 for the defect along the width).

Figure 63 compares all configurations for a defect along the length. Overall, all the defects show an improvement. The gap configuration has reached 13% enhancement and this is closely followed by half gap/overlap (10%) and overlap (7%). This improvement in the mechanical property is controlled by a more severe delamination all around the hole. Indeed, the defect creates a weak spot along the length that allows the cracks to propagate easily at this location. Combined with the stress concentration factor, created by the hole (highest stress along the width), the entire hole circumference is weakened and allows cracks to propagate easily. For all samples with a defect, more cracks propagate around the hole compared with the baseline configuration, consequently, it increases the effect formulated by Suemasu et al.[21], and improves the ultimate

strength. However, the delaminations reduce the integrity of a laminate. This form of defect that fails the inspection must be considered for a composite structure design.
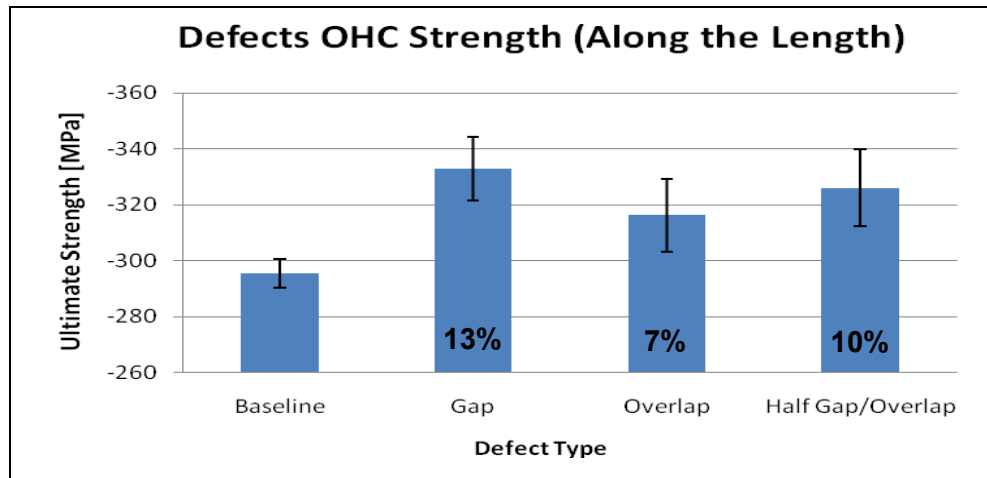
Figure 63: OHC Strength variation as a function of the defect type along the length

Figure 64 compares the configurations with a defect along the width. Unlike the previous defect orientation, this one shows opposite results. The different layups for this test do not change the general behaviour of the ultimate strength, but affect its amplitude. For the same ratio of angle plies and a small difference in stacking sequence, the baseline strength has increased of about 25 MPa (8%). All the defect configurations show up to 12% decrease in the ultimate strength with the maximum degradation for the half gap/overlap configuration, followed by both gap and overlap with 9%. The defect along the width increases the effect of the stress concentration and initiates the cracks earlier. On all these samples, the delamination has not appeared as significant as the other defect orientation, and did not propagate around the entire hole circumference. In other words, cracks have started at the weak spot with higher stress concentration before propagating along the defect without presenting much delamination.
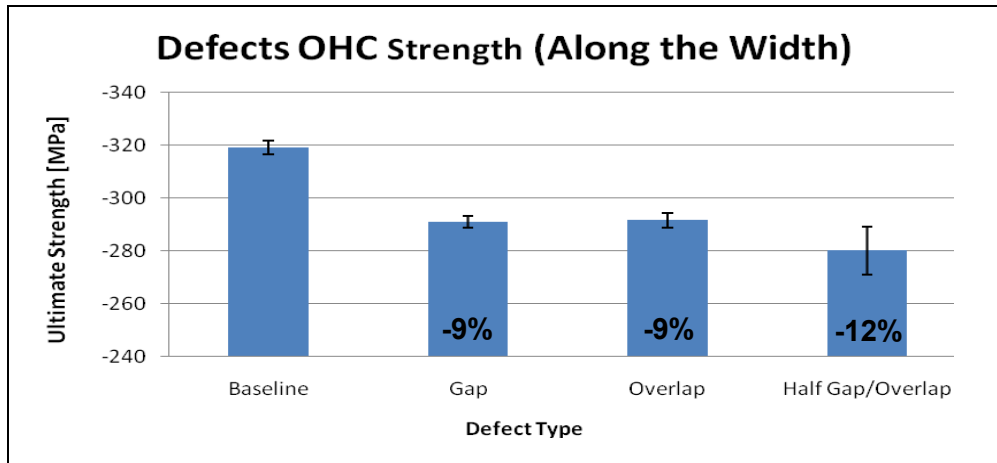
Figure 64: OHC Strength variation as a function of the defect type along the width

5.2.7   Results summary

All these last tests and observations have allowed a better understanding of the different defect configurations. In general, the micrographs have shown the excellent ply consolidation obtained with this process. Also, for a unidirectional laminate, the tows will move to accommodate all defects shape without inducing too much resin rich areas. On the other hand, for a 0-90° or a quasi-isotropic laminate, the angle between two consecutive layers will affect the gap size and, consequently, the resin rich area size. Also, the overlap geometry does not change according the stacking sequence and keep its fiber waviness more constant throught its thickness than the gap configuration. Overall, the smallest radius of curvature associated with the half gap/overlap configuration affect the fiber waviness and the compression properties.

In fact, all tests have helped provide a guideline: the lamina level is less affected by the different defects than the laminate level, which has shown lower variations on the ultimate strength. At the lamina level, the maximum overall reduction is less than 5% except for the in-plane shear test with an overlap and a half gap/overlap located along the width. Also, the Open Hole Tension test suggests that the stress concentration, generated by the hole, influences more the ultimate strength than the different defects. On the other hand, the defect orientation in the Open Hole Compression influences the failure mechanism by increasing the delamination and, consequently, the ultimate strength. The tests carried out in this work help to gain insight into the failure mechanism behaviour of samples

manufactured with the AFP process. Figure 65 summarize the results in a visual fashion to provide design guideline. A variation of ±3% is assumed negligible and is represented by a black line. The arrows represent an increase or a decrease of more or equal than 3%.

		Gap	Overlap	Half Gap/Overlap	Twisted Tow
Tension		—	—	↘	↗
Compression		—	↗	—	—
In-Plane Shear	Length	—	—	↘	↘
	Width	↗	↘	↘	↘
OHT		—	—	—	
OHC	Length	↗	↗	↗	
	Width	↘	↘	↘	

↗ ≥ 3% increase (up to 13%)

— ±3% variation

↘ ≥ 3% decrease (up to 12%)

Figure 65: defects comparison chart

Figure 65 provides a guideline for establishing the next set of experiments and requirements for manufacturing composite parts assisted by the AFP process. It is shown that a defect sometime improves the ultimate strength but, overall for a particular defect, an improvement in a mechanical property brings a reduction for another one. It is difficult for a real part with multidirectional loadings to exploit the advantage of a mechanical property increase. The three defects that cause the most overall damage are gap, overlap and half gap/overlap. However, the highest thicknesses variations brought by the overlap configuration create poor aerodynamics properties and, also, is more difficult to manufacture with close tolerances. Therefore, aeronautic companies tend to reject this defect configuration and adopt the "no overlap" rule. From the previous tests, many defect configurations show near-negligible results, which suggest that the defect distribution should be considered, and that one defect alone does not have large impact.

CHAPTER 6: Conclusion

This experimental investigation has helped to understand the impact of the defects that occurs during the manufacturing of composite structures by the Automated Fiber Placement (AFP) process. The experiments have shown that the lamina level is less affected by the presence of a defect than the laminate level with a maximum strength reduction of 5% compared to 13%. For this reason, more effort is required to understand the behaviour of laminates.

Results have shown that the Open Hole Tension failure is mostly influenced by the stress concentration than by the defect itself. On the other hand, the Open Hole Compression test is influenced by the defect orientation which affects the failure mechanism and gives different results. A defect through the width (90°) increases the stress concentration effect and, consequently, reduces the ultimate strength. In contrast, a defect along the length (0°) creates a weak region at its intersection and the edge of the hole, which facilitated the delamination. The failure is still initiated along the width, but propagates more easily around the hole, thus increasing the delamination size in the vicinity of the hole and increases the ultimate strength (toughening mechanism). In general, the main failure mechanism of all compression specimens was found to be the fiber waviness in the loading direction because it induces the micro-buckling and, consequently, earlier failure. This observation is supported by micrographs that helped in understanding the real geometrical changes after cure and can help to create more accurate numerical analysis.

Finally, a global prediction approach that account for the experimental results was described in order to obtain a more accurate model. With this tool, companies would be able to reduce the uncertainties associated with this process, to complete more easily qualification process and to have more flexibility during the design process.

CHAPTER 7: Future Work

From the previous experiments, the compression tests (fiber compression and open hole compression) have seen the highest strength reductions with the insertion of different defects. These strength reductions were mainly the consequence of the fiber waviness induced by the defect on the other layers, which initiates earlier micro-buckling. Also, the near negligible results suggest that a single defect does not have significant impact on the ultimate strength. Considering that this process randomly induces the defects in the entire structure and that we know the basic impact of a single defect, it is now more appropriate to investigate the impact of the defect distribution.

In order to analyse the impact of the distributed defects, two different distributions can be investigated: through the area and through the thickness. An area distribution of defects helps to scale the impact on larger structures and to see the accumulation of these impacts. On the other hand, a distribution of defects throught the thickness helps to obtain the worst-case scenario at the coupon scale by combining the effects, e.g. fiber waviness, at the same location and is also more suitable for small specimens' size.

At the coupon scale, the previous tests give the minimum impact induced by a single defect. Similarly, a distribution of defects throught the thickness should combine these effects in order to obtain the maximum value of impact. Furthermore, with these two different results, it would be possible to find the range of impact induced locally by the defects. For all kind of defects, the range can be found at both the lamina and laminate level but, as shown previously, the laminate level should show the highest effect. In order to consider all possible cases and from a qualification point-of-view, these steps should be executed for different loading (static, fatigue and impact) and for different environments (humidity and temperature).

After understanding the impact at a small scale, it will be possible to distribute alternative defects on a larger area (panel). The configuration that gives the highest impact at the coupon size can be implemented for different density of defect with the aim of capturing the worst-case scenario. Then, to validate the

experimental results, a Finite Element Analysis (FEA) should be performed for both coupon and panel size to find their corellations and obtain better predictions.

Both coupon and panel scales are useful to predict the real behaviour of a complex shape and a variable stiffness part. The lamina properties at the coupon scale should be useful during the ply definition of a prediction code, while the laminate properties at the panel scale should be used during the failure criterion definition depending on the constraints and loading factors.

Figure 66 shows a possible way to analyse a complex variable stiffness part considering the impact of the defects. First, an optimization can be done to find the best layup considering the machine constraints and loadings. Second, a tow courses prediction gives the real position of the defects and their density. Third, the part is split into many elements and the stacking sequence is assigned independently for all of them depending on the coordinate and the defect location. For each element, a straight fiber approximation is used to simplify the analysis. Consequently, the smaller are the elements, the more accurate is the approximation. At this step, the lamina properties of the defects should be taken into account in the staking sequence definition for each element. Then, depending on the density of defects, the stacking sequence and the constraints (open hole, filled hole, etc.), the ultimate strengths are applied in the failure criterion (the worst case scenario is more conservative). For complex parts with different constraints or with curvinear fiber paths, the part should be split in several subsections with a failure criterion adapted to each situation.

By including the impact of defects in the entire analysis, the solution will be more accurate because all phenomena are taken into account, including the fiber waviness and the random defects induced by the machine that cannot be avoided. As demonstrated in previous sections, the fiber waviness plays a major role in the failure mechanism, especially in compression, and is dependent on the size and the nature of the defect. In addition, it was demonstrated that the resin rich area depends on the defect size and the ply angle of other layers. So, the actual approximation that all fibers stay straight (out-of-plane) and the assumption that the gap area is filled by resin is not an accurate estimation and, consequently, the safety factor might need to be increased. It was demonstrated

for a notched laminate with a single defect, that the strength can reduce by about 12% and the estimated reduction for a configuration with more defects should be even higher; therefore, the failure criterion must be taken into account.

Large scale prediction including the impact of the defects

Fiber path optimization

Levend Parnas, Süha Oral, Ümit Ceyhan [2003]

Tow courses prediction and density of defect

Tow drops

Gap regions

Overlap regions

Zafer Gürdal, Brian F. Tatting and K. Chauncey Wu [2005]

FEA mesh on each subsection (Assuming straigth fiber in each element)

Levend Parnas. Süha Oral. Ümit Cevhan [2003]

Material Properties reduction due to defects (Defect analisys)

- Lamina properties: Stacking sequence definition

- Laminate properties (worst case): Failure criterion

Impact at the coupon level

Mechanical Properties

types of defect

Maximum Impact at the panel level

Mechanical Properties

types of defect

Structure prediction

The complex structure should be divided into subsections. In each subsection, the ultimate strength is ajusted independently, for each axis, in order to represent the real case (density, stress concentration, layup, etc.).
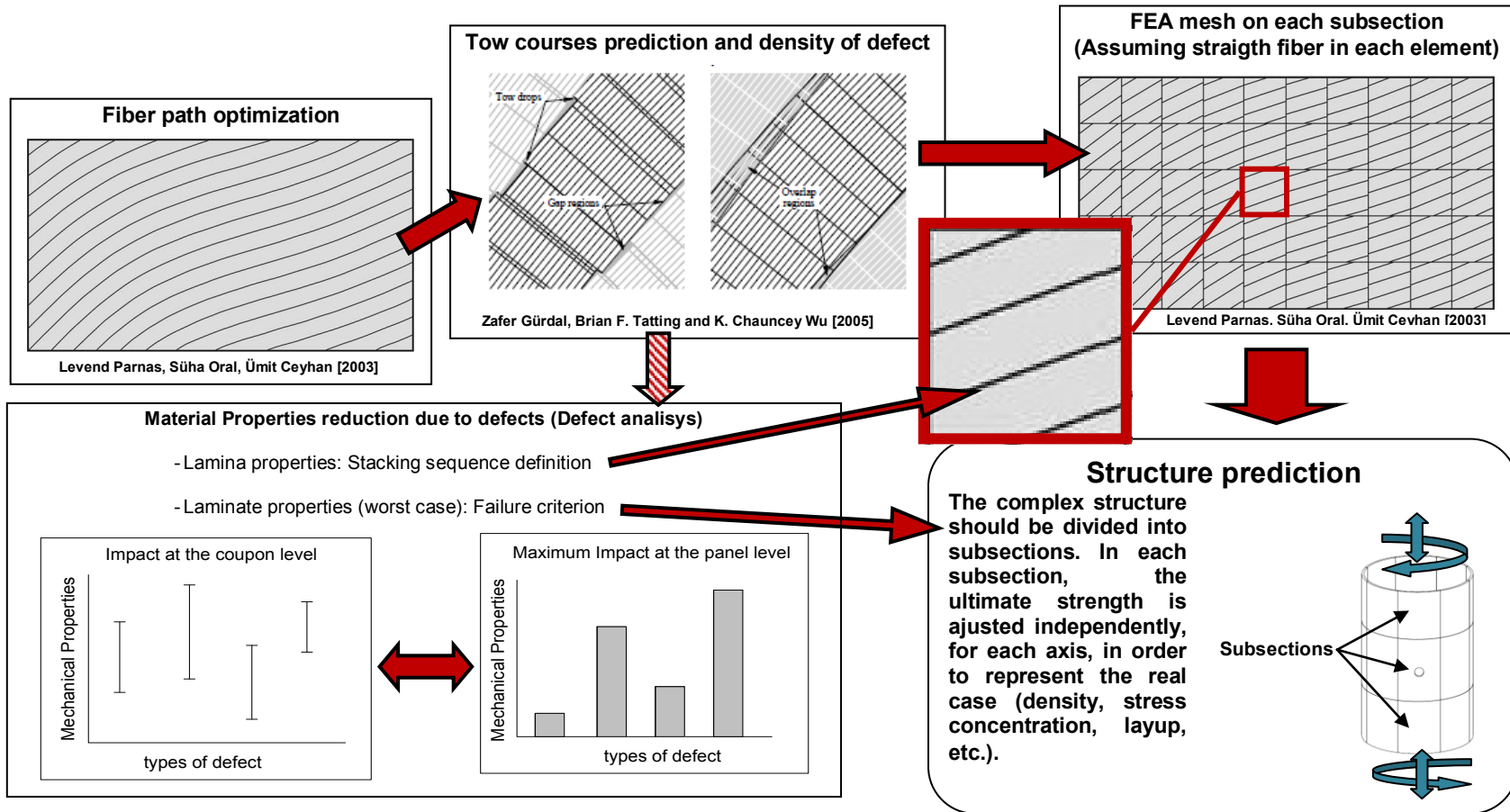
Subsections

Figure 66: Analysis on a real structure considering the defects

References

1. Daniel, Isaac M. & Ishai, Ori, "Engineering Mechanics of Composite Materials", 2005, pp. 529

2. Lee, Stuart M., "Handbook of Composite Reinforcements", 1992, pp. 715

3. Gurdal, Zafer, et al., "Tow-Placement Technology and Fabrication Issues for Laminated Composite Structures", *46th AIAA/ASME/ASCE/AHS/ASC Structures, Structural Dynamics and Materials Conference*, Austin, Texas, 2005, April 18-21, pp. 18

4. Wu, K. Chauncey, et al., "Structural Response of Compression-Loaded, Tow-Placed, Variable Stiffness Panels", *43th Structural Dynamics and Materials Conference*, Denver, Colorado, 2002, April 22-25, pp. 22

5. Gurdal, Zafer, et al., "Variable stiffness composite panels: Effects of stiffness variation on the in-plane and buckling response", *Composites Part A: Applied Science and Manufacturing* 5, 2008, pp. 911-922

6. Tatting, Brian F. & Gurdal, Zafer, "Design and Manufacture of Elastically Tailored Tow Placed Plates", NASA Langery Reasearch Center, NASA/CR-2002-211919, 2002, pp. 34

7. Cairns, Douglas S., et al., "Response of Automated Tow Placed Laminates to Stress Concentrations", *Third NASA Advanced Composites Technology Conference*, United States, 1993, pp. 649-663 (SEE N95-28823 10-24)

8. Blom, Adriana W., et al., "Design of Variable-Stiffness Conical Shells for Maximum Fundamental Eigenfrequency", *Comput. Struct.* 9, 2008, pp. 870-878

9. McManus, Hugh L. & Mak, Yew-Po, "Strain Rate and Manufacturing Technique Effects on the Damage Tolerance of Composite Laminates", *Structural Dynamics and Materials Conference*, La Jolla, CA, 1993, Apr. 19-22, pp. 853-1862

10. Sawicki, Adam J. & Minguet, P. J., "The Effect of Intraply Overlaps and Gaps Upon the Compression Strength of Composite Laminates", *39th AIAA Structural, Dynamics, & Materials Conferences*, Long Beach, CA, 1998, April, pp. 744-754

11. Donaldson, Daniel B. Miracle and Steven L., "ASM handbook: Composites", Material Parc, Ohio, 2001, pp. 1201

12. Measom, Ronald & Sewell, Kevin, "Fiber Placement Low-Cost Production for Complex Composite Structures", *American Helicopter Society 52nd Annual Forum*, Washington, DC, 1996, June 4-6, pp. 12

13. Blom, Adriana W., et al., "A Theoretical Model to Study the Influence of Tow-drop Areas on the Stiffness and Strength of Variable-stiffness Laminates", *Journal of Composite Materials* 5, 2009, pp. 403-425

14. Iarve, E. V. & Kim, R., "Strength Prediction and Measurement in Model Multilayered Discontinuous Tow Reinforced Composites", *Journal of Composite Materials* 1, 2004, pp. 5-18

15. Turoski, Luke Everett, "Effects of Manufacturing Defects on the Strength of Toughened Carbon/Epoxy Prepreg Composites", Montana State University, Bozeman, July, 2000, pp. 125

16. ASTM D3039/D3039M, "Standard Test method for Tensile Properties of Polymer Matrix Composite Materials", American Society for Testing and Materials, Philadelphia, 2006

17. ASTM D3410/D3410M, "Standard Test method for Compressive Properties of Polymer Matrix Composite Materials with Unsupported Gage Section by Shear Loading", American Society for Testing and Materials, Philadelphia, 2006

18. ASTM D5379/D5379M, "Standard Test method for Shear Properties of Composite Materials by the V-Notched Beam Method", American Society for Testing and Materials, Philadelphia, 2006

19. ASTM D5766/D5766M, "Standard Test method for Open Hole Tensile Strength of Polymer Matrix Composite Laminates", American Society for Testing and Materials, Philadelphia, 2006

20. ASTM D6484/D6484M, "Standard Test method for Open Hole Compressive Strength of Polymer Matrix Composite Laminates", American Society for Testing and Materials, Philadelphia, 2006

21. Suemasu, H., et al., "On failure mechanisms of composite laminates with an open hole subjected to compressive load", *Composites Science and Technologiy* 66, 2006, pp. 634-641

APPENDIX A:

Expected maximum strength reduction at the coupon level: Details of the test plan

Time and material constraints have cut short the planned tests and, consequently, only the lowest effect tests have been performed. The following proposed second set of tests would find the worst-case scenario (maximum reduction) at the coupon level for two loading cases: compression and OHC. So, the test plan is presented for a better understanding of this method.

From the previous results, the compression tests have shown more influence on material properties when manufacturing defects are present. Consequently, the following experiments should be conducted for both compression and open hole compression at the laminate level, and with the same quasi-isotropic layup that was used by the previous OHC test (following the ASTM standard: [45/-45/90/0]2S). Moreover, at the laminate level, straight fibers panels are easier to manufacture, evaluate with a baseline configuration (without defects) and to implement during a qualification process. Also, most aeronautic laminates are made with a quasi-isotropic layup, again motivating our choice of laminate. As said previously, a variable stiffness laminate is approximated as straight fibers when a small mesh is used during the FEA analysis. Consequently, an investigation based on straight fibers is appropriate to understand the impact and, afterwards, can be applied to variable stiffness laminates; to reduce the error many stacking sequence should be tested. In addition, the laminate used during the test should be the same as the laminate used during the design because the testing results will be used in the failure criterion.

a)

b)

TOP VIEW

45° LAYER (NO DEFECT)
-45° LAYER (NO DEFECT)
90° LAYER (WITH DEFECT)
0° LAYER (NO DEFECT)
45° LAYER (WITH DEFECT)
-45° LAYER (WITH DEFECT)
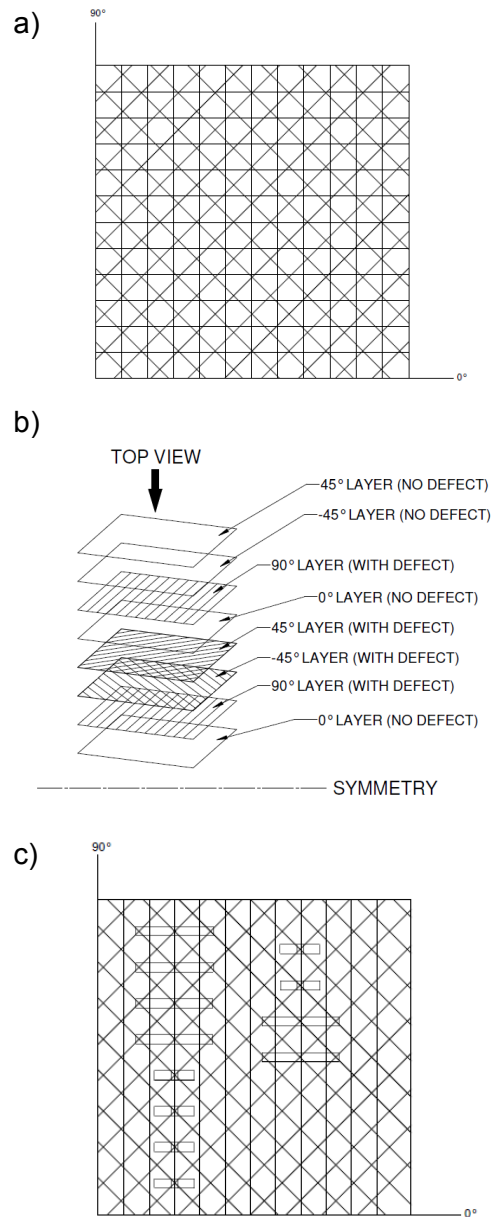90° LAYER (WITH DEFECT)
0° LAYER (NO DEFECT)

SYMMETRY

c)

Figure 67: Coupons configuration; a) Quasi-isotropic grid; b) Defect configuration; c) Coupons placement

During his experiments, Luke Everett Turoski [15] found that a 3-defect configuration gives the highest strength reductions (4-defects configurations obtained almost the same reduction as the 3-defect configuration). So, based on his results and our first set of tests, the estimated maximum reduction (worst case scenario) should be obtained during the 3 defect configuration (defects situated in the 90°, +45° and -45° layers). Also, based on E. V. Iarve and R. Kim [14] and in order to avoid crack initiation in the top and bottom ±45° layers, these layers should not contain any defects. This method (top and bottom ±45° layers without defect) has been adopted because it minimizes the general impact of the defects, so it is more representative to real designs.

Two similar quasi-isotropic grids are proposed (Figure 67a), one containing gaps and the other containing overlaps (the lines represent the defects). Also, the defects were assigned to selected layers (Figure 67b), and marks should be created on the panel, before the cure process, to indicate the location of the defects. From these marked locations, coupons should be cut so that the defect intersections are located in the middle of the test sections (Figure 67c). Then, each sample should be tested and compared with a baseline configuration without defect. The following sections will discuss the specimen geometries and the test issues for both compression and open hole compression specimens.

Defect Geometry

In order to spread the defects inside different layers and through the entire thickness, the defects cannot be made by modifying two stacked tows, like in the previous tests. Consequently, the geometry of the defects is slightly different. For the gap configuration, only one tow is removed at the specified locations on the grid and only on the selected layers (Figure 67b). The overlap configuration is similar to the gap configuration, but only one tow is added, instead of removed. So, for both 16-ply configurations, eight layers contain the defects and eight layers are exempt of defects.

Test description

The compression test is executed in the same way as the previous tests, and is made with the same OHC quasi-isotropic layup. Also, this layup can be adjusted to the real quasi-isotropic layup used by each company (soft, quasi and hard layup). In order to capture the effect of the defects without edge effects, the specimen width and the test length have been increased. Figure 68a represents the geometry of the modified compression specimen. For compression tests, attention is required to avoid buckling in the test section, which is a function of the thickness, the predicted ultimate strength, the stiffness, the test gage length and the width of the specimen. Also, the 45° defect, for this configuration, creates a relation between the test length and the width of the specimen (Figure 68a) and, consequently, the test length is related to the width. To verify the feasibility of this proposal, three preliminary tests, without the anti-buckling feature, were executed on a baseline 16 ply laminate at different specimen widths: 25mm (35mm test length), 30mm (39mm test length) and 36mm (55mm test length). All these specimens showed a mode 1 buckling response before breaking. Consequently, to obtain pure compression failure, with our material, the thickness should be almost twice its actual thickness (around 32 plies).

The Open Hole Compression geometry, dictated by the ASTM standards, is still suitable for this defect configuration (Figure 68b). For this test, buckling is not an issue because the fixture has an anti-buckling feature, so, the dimensions are the same that the last OHC tests and the only changes are the location of the defects.
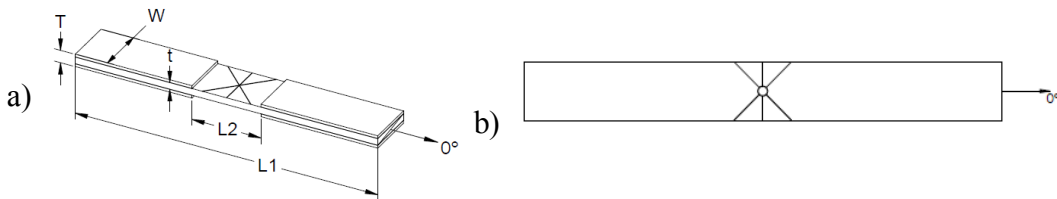

Figure 68: Specimen geometry (quasi-isotropic layup); a) Modified Compression; b) OHC